

230151

WISCONSIN WRD DISTRICT
LIBRARY COPY

A RAINFALL-RUNOFF MODELING PROCEDURE FOR IMPROVING ESTIMATES OF T-YEAR (ANNUAL) FLOODS FOR SMALL DRAINAGE BASINS

U.S. GEOLOGICAL SURVEY

Water-Resources Investigations 78-7



BIBLIOGRAPHIC DATA SHEET	1. Report No.	2.	3. Recipient's Accession No.
4. Title and Subtitle A rainfall-runoff modeling procedure for improving estimates of T-year (annual) floods for small drainage basins			5. Report Date August 1978
7. Author(s) R. W. Lichty and F. Liscum			6. 8. Performing Organization Rep No. USGS/WRI 78-7
9. Performing Organization Name and Address U.S. Geological Survey Water Resources Division Denver Federal Center, Box 25046 Lakewood, CO 80225			10. Project/Task/Work Unit No.
12. Sponsoring Organization Name and Address U.S. Geological Survey Water Resources Division Denver Federal Center, Box 25046 Lakewood, CO 80225			11. Contract/Grant No. 13. Type of Report & Period Covered Final
15. Supplementary Notes			14.
16. Abstracts Maps depicting the influence of a climatic factor, <i>C</i> , on the magnitude of synthetic T-year (annual) floods were prepared for a large portion of the eastern United States. The climatic factors were developed by regression analysis of flood data generated using a parametric rainfall-runoff model and long-term rainfall records. Map estimates of <i>C</i> values and calibrated values of rainfall-runoff model parameters were used as variables in a synthetic T-year flood relation to compute "map-model" flood estimates for 98 small drainage basins in a six-state study area. Improved estimates of T-year floods were computed as a weighted average of the map-model estimate and an observed estimate, with the weights proportional to the relative accuracies of the two estimates. The accuracy of the map-model estimates was appraised by decomposing components of variance into average time-sampling error associated with the observed estimates and average map-model error. Map-model estimates have an accuracy, in terms of equivalent length of observed record, that ranges from 6 years for the 1.25-year flood up to 30 years for the 50- and 100-year flood.			
17. Key Words and Document Analysis. 17a. Descriptors Floods, climatic data, rainfall-runoff relationships, synthetic hydrology, regression analysis, regional analysis			
17b. Identifiers/Open-Ended Terms			
17c. COSATI Field Group			
18. Availability Statement		19. Security Class (This Report) UNCLASSIFIED	21. No. of Pages 44
No restriction on distribution		20. Security Class (This Page) UNCLASSIFIED	22. Price

A RAINFALL-RUNOFF MODELING PROCEDURE
FOR IMPROVING ESTIMATES OF T-YEAR (ANNUAL)
FLOODS FOR SMALL DRAINAGE BASINS

By R. W. Lichty and F. Liscum

U.S. GEOLOGICAL SURVEY

Water-Resources Investigations 78-7



August 1978

UNITED STATES DEPARTMENT OF THE INTERIOR

CECIL D. ANDRUS, Secretary

GEOLOGICAL SURVEY

H. William Menard, Director

For additional information write to:

U.S. Geological Survey
Water Resources Division
Box 25046, Denver Federal Center
Denver, Colorado 80225

CONTENTS

	Page
Abstract-----	1
Introduction-----	2
Methods of study-----	3
Rainfall-runoff model-----	4
Selection of model calibration sites-----	5
Synthesis of annual floods-----	5
Formulation of multiple-regression model-----	7
Regression analysis of synthetic T-year floods--rural model applications-----	8
Effects of imperviousness on synthetic floods-----	11
Single-coefficient relation for synthetic T-year floods-----	12
Geographic variability of climatic factor, C -----	14
Map-model estimates of T-year floods at calibration sites-----	18
Comparison of observed and map-model flood estimates-----	21
Accuracy and weighting of observed and map-model T-year floods-----	23
Summary and conclusions-----	31
References-----	33

ILLUSTRATIONS

Figure 1. Schematic outline of model structure, showing components, parameters, variables, and input/output data-----	4
2. Map showing locations of long-term rainfall, and small streams, calibration sites used in study-----	6
3. Relationship between regression constant, a_i , and regression coefficient, b_{2_i} -----	10
4. Relationship between the coefficients a_i , and d_i -----	13
5. Contour map showing the geographic variation in the 2-year recurrence interval climatic factor, C_2 -----	15
6. Contour map showing the geographic variation in the 25-year recurrence interval climatic factor, C_{25} -----	16
7. Contour map showing the geographic variation in the 100-year recurrence interval climatic factor, C_{100} -----	17
8. Scatter diagrams of observed and map-model T-year flood estimates-----	22
9. Trends in error-variance components as a function of recurrence interval-----	29

TABLES

		Page
Table 1.	Model parameters and variables and their application in the modeling process-----	35
2.	Long-term recording rainfall sites used in study-----	36
3.	Streamflow stations used in study-----	37-40
4.	Results of multiple-regression analyses for rural model applications-----	41
5.	Summary and comparison of multiple-regression (<i>m-r</i>) and direct-search (<i>d-s</i>) determinations for the coefficient, α_i -----	42
6.	Results of the direct-search determinations for the coefficient d_i for effect of impervious area-----	43
7.	Standard errors for the single-coefficient, synthetic flood relation-----	44

A RAINFALL-RUNOFF MODELING PROCEDURE FOR IMPROVING ESTIMATES OF
T-YEAR (ANNUAL) FLOODS FOR SMALL DRAINAGE BASINS

By R. W. Lichty and F. Liscum

ABSTRACT

The U.S. Geological Survey rainfall-runoff model is used to synthesize a sample of 550 annual-flood series, that are representative of both rural- and impervious-area model applications, using data from each of 36 long-term recording rainfall sites. A flood-frequency curve is developed for each annual-flood series, and a single-coefficient, regression relation for the 2-, 25-, and 100-year floods is developed for each one of the rainfall sites-- a generalized definition of the model output as a function of the model parameters for each rainfall site. The site-to-site variability in the magnitude of the coefficient that characterizes the synthetic T-year (annual) flood relation is interpreted as reflecting the spatially varying influence of local climatic factors, C_i , on the results of synthesis. Three contour maps that depict the geographic variability of the climatic factor were prepared. Estimates of the C_i values taken from these maps were used in conjunction with fitted rainfall-runoff model parameters and the synthetic T-year flood relation to develop map-model, T-year flood estimates for 98 rural-area streamflow stations located in Missouri, Illinois, Tennessee, Mississippi, Alabama, and Georgia. Comparisons of these flood estimates with those based on observed annual floods show that the map-model estimates are generally lower than the observed estimates for return periods greater than the 2-year recurrence interval. This tendency to underestimate the higher recurrence interval floods was removed by use of an average adjustment factor, B_i , and the average accuracy of "unbiased", map-model flood estimates was appraised for the test sample of 98 streamflow stations. The accuracy of the map-model estimates increases rapidly with increasing recurrence interval up to the 10-year interval, and then reverses its trend and decreases slowly. The map-model flood estimates are more accurate beyond the 10-year recurrence interval than observed estimates based on a harmonic-mean record length of 13.2 years.

Improved T-year flood estimates were computed by weighting observed and map-model estimates, and the accuracy of the improved estimates is appraised as a function of recurrence interval, and in terms of the concept of

equivalent length of record. The map-model estimating procedure yields an equivalent length of record that ranges from a low of about 6 years for the 1.25-year flood, up to an ultimate, maximum level of about 30 years of data for estimating the 50- and 100-year recurrence interval floods.

INTRODUCTION

Historically there has been a deficiency of flood data for drainage basins smaller than about 50 square kilometers. Yet the need for such data is great because accurate and timely estimates of the magnitude and frequency of T-year (annual) floods are an important consideration in the design of drainage structures and the delineation of flood-prone areas. The U.S. Geological Survey, in cooperation with various State, Federal, and local agencies, has undertaken an extensive program of data collection to develop a better knowledge of the flood-frequency characteristics of small basins.

Many years of annual flood data are required to reliably define a flood-frequency curve. One procedure utilized by the Survey to estimate T-year floods from short records is rainfall-runoff modeling. Rainfall-runoff modeling is undertaken because relatively long records (60 to 70 years) of rainfall are available at many locations throughout the country. Basically, the concept is that the information contained in the long-term rainfall records can be transformed to streamflow information by synthesizing a long record of annual floods using a calibrated rainfall-runoff model, such as that developed by Dawdy, Lichty, and Bergmann (1972). That is, a short record of observed floods can be effectively lengthened, and the time-sampling error inherent in small samples can be reduced, by the rainfall-runoff modeling process.

A major problem associated with this type of rainfall-runoff model application is the lack of long-term rainfall data at each site for which model-extended data are required or desired. The goal of reducing time-sampling error in observed flood-frequency estimates can, in general, only be achieved if a method of integrating and transferring information from the available long-term rainfall sites is incorporated in the modeling procedure. In addition, the accuracy of the transfer mechanism must be appraised to allow a meaningful weighting of observed and modeled flood-frequency estimates in relation to their respective accuracies.

This report describes and evaluates a procedure for computing improved estimates of T-year floods that incorporates a rainfall information transfer mechanism in the form of three maps, and a generalized definition of synthetic T-year flood potential as a function of fitted rainfall-runoff model parameters. The maps depict the geographic variability of a coefficient, C_i , ($i = 2-, 25-, \text{ and } 100\text{-year recurrence intervals}$) that reflects the influence of local climatic factors on synthetic T-year floods. The climatic factors are derived by analysis of the results of synthesis using the rainfall-runoff model in conjunction with long-term rainfall data and an average daily pattern of potential evapotranspiration.

The generalized definition of synthetic T-year floods facilitates the computation of a "map-model", flood-frequency curve at small-basin calibration sites by using map estimates of the climatic factor, C_i , and fitted rainfall-runoff model parameters. Comparisons of observed and map-model, T-year, flood estimates, for a sample of 98 rural-area calibration sites located in Missouri, Illinois, Tennessee, Mississippi, Alabama, and Georgia, show that the map-model estimates are generally too low in relation to observed estimates for recurrence intervals greater than the 2-year or median flood. Average bias correction factors, B_i , are determined for the 2-, 25-, and 100-year recurrence intervals, and the accuracy of "unbiased", map-model, T-year flood estimates is evaluated by decomposing error variance components into average error variance of the map-model estimates, and average time-sampling error variance associated with the observed flood estimates.

The procedure for computing an improved T-year flood estimate involves the computation of a weighted average of the observed and map-model estimates. The weighting factors are developed for each calibration site as a function of the time-sampling variance of the observed estimate and the average variance of the map-model estimate.

METHODS OF STUDY

Many flood-frequency investigations have successfully utilized multiple-regression analysis to explain the variability in the occurrence of floods, and to provide a generalized definition of the magnitude of T-year floods as a function of drainage-basin characteristics. For example, Benson (1962, 1964) and Thomas and Benson (1970) demonstrated that observed T-year flood estimates may be related to various topographic and climatic factors (basin characteristics) in the form

$$\hat{Y} = \alpha X_1^{b_1} X_2^{b_2} \dots X_n^{b_n}, \quad (1)$$

where

\hat{Y} = predicted value of T-year flood,

X_1 to X_n = basin and climatic characteristics (drainage area, slope, precipitation intensity, and so forth),

α = regression constant, and

b_1 to b_n = regression coefficients.

In an analogous manner, multiple-regression analysis should be useful in explaining the variability of synthetic floods derived by rainfall-runoff modeling using a particular long-term rainfall record. It should also provide

a generalized definition of the magnitude of synthetic T-year floods, as a function of rainfall-runoff model parameters, for each individual rainfall site. Study and interpretation of the regression results should provide insight into how the influence of climate manifests itself in the magnitude, interaction and geographic variability of the regression constant and coefficients, a, b_1, b_2, \dots, b_n .

Rainfall-Runoff Model

The rainfall-runoff model used in this study is a simplified, conceptual, bulk-parameter, mathematical model of the surface-runoff component of flood-hydrograph response to storm rainfall. (Dawdy, and others, 1972.) The contribution of base flow, interflow, and quick return flow to the flood hydrograph are not considered because they are generally negligible. The model deals with three components of the hydrologic cycle--antecedent soil moisture, storm infiltration, and surface-runoff routing. The first component simulates soil-moisture conditions at the onset of a storm period through the application of moisture-accounting techniques on a daily cycle. Estimates of daily rainfall, evaporation, and initial values of the moisture storage variables are elements used in this component. The second component involves an infiltration equation (Philip, 1954) and certain assumptions by which rainfall excess is determined on a 5-minute accounting cycle from storm-period rainfall. Storm rainfall may be defined at 5-, 10-, 15-, 30-, or 60-minute intervals, but loss rates and rainfall excess amounts are computed at 5-minute intervals. The third component transforms the simulated time pattern of rainfall excess into a flood hydrograph by translation and linear storage attenuation (Clark, 1945.) The structure of the model is shown in figure 1 (following). Table 1 (page 35) summarizes the model parameters and their application in the modeling process; (all tables are at end of report). For a more complete description of the model see Dawdy, Lichty, and Bergmann (1972).

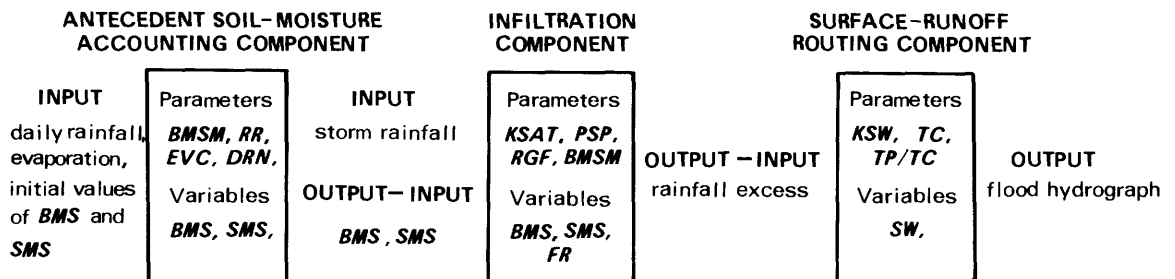


FIGURE 1: - Schematic outline of the rainfall-runoff model structure, showing components, parameters, variables, and input-output data, flow is left to right.

The model and an automated procedure for determining optimal parameter values are included in both FORTRAN and PL/1 computer language programs, described by Carrigan (1973). The programs provide for the input and storage of observed data, the simulation of flood hydrograph response to storm rainfall, and multistep optimization of model parameters to minimize the error between observed and computed flood peaks.

Selection of Model Calibration Sites

Model calibration results were assembled for sites in Missouri (Hauth, 1974), Alabama (McCain, 1974), Mississippi (Colson and Hudson, 1976), Georgia (Golden and Price, 1976), Tennessee (Wibben, 1976), and Illinois (Curtis, 1977), and a sample of 99 streamflow stations was selected to give an approximately uniform spatial configuration of station locations over the six-state study area (fig. 2). Calibrations were rerun for sites in Missouri, Tennessee, Alabama, and Georgia, to conform to a restrictive set of calibration guidelines, as follows, assign *RR*, *EVC*, *DRN*, and *TP/TC* (table 1). Recalibration results were essentially the same as those initially reported. The sample was divided into two sets: 50 stations for development of synthetic annual-flood data, and the remainder withheld, to be included in the development and evaluation of a map-model estimating procedure.

Synthesis of Annual Floods

At each of the 36 long-term rainfall sites shown in figure 2, and described in table 2, synthetic data were developed to relate rainfall-runoff model estimates of T-year floods to the parameters of the model. This was accomplished by generating a sample of 50 synthetic, annual-flood series using data from each rainfall site. The synthetic data sets were developed using calibrated model parameters for a representative sample of 50 basins shown in figure 2, and described in table 3. Replicate synthesis was performed at each rainfall site using the same sample of fitted model parameters, resulting in a total of 1,800 synthetic, annual-flood series (50 parameter sets by 36 rainfall records) that are representative of model applications in small rural basins.

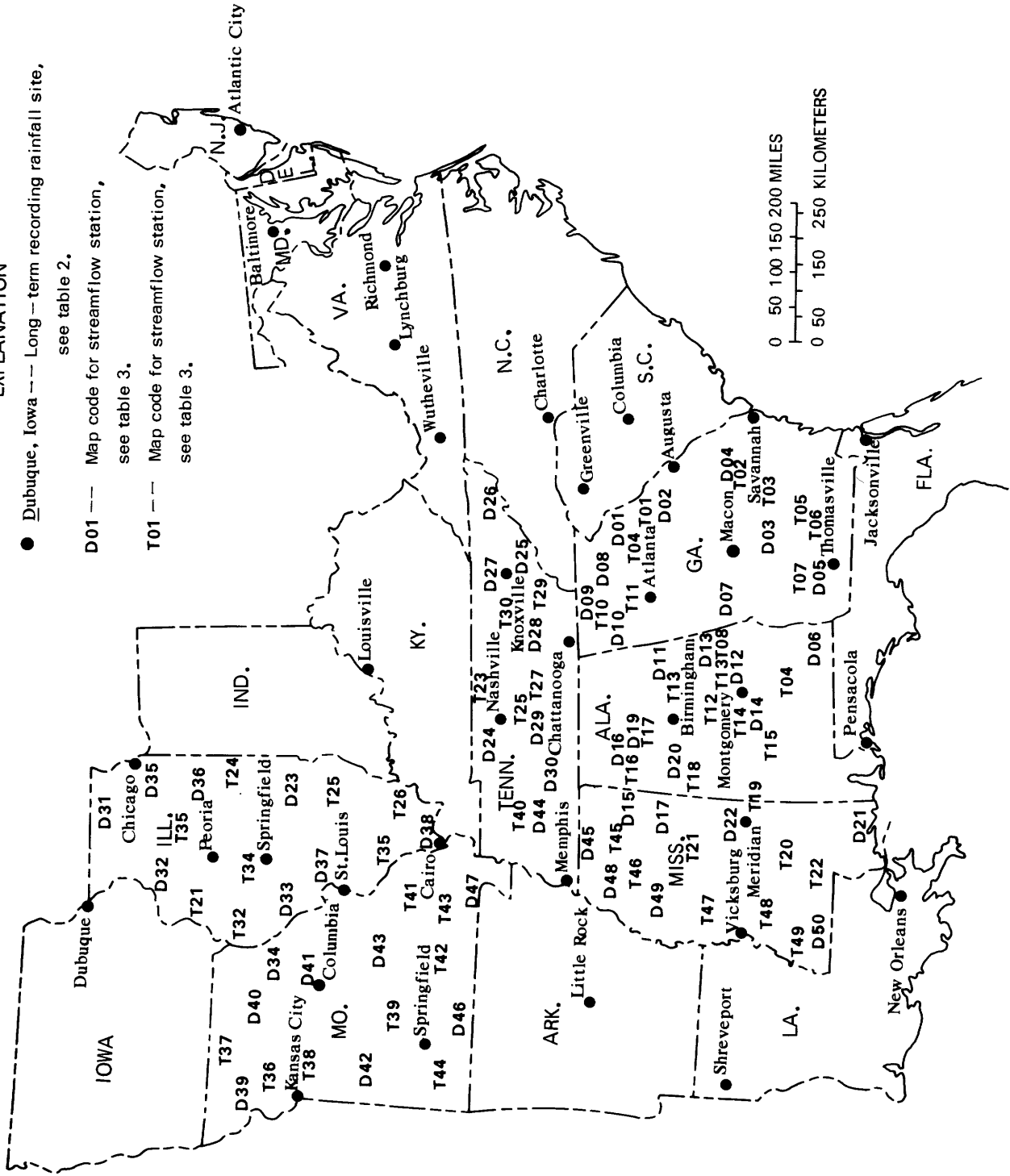
Additional flood series were generated in an analogous manner to study the effects of "urban development" on synthetic flood characteristics. Ten levels of imperviousness (5, 10, ..., 50 percent) were assigned to each model/rain-gage application, resulting in a total of 18,000 (50 by 36 model/rain-gage applications by 10 levels of imperviousness) synthetic, annual-flood series with impervious effects. The generation of rainfall excess from impervious surfaces was modeled by a simple threshold concept that required the retention of 0.05 inch of storm rainfall before the surface becomes 100 percent effective in producing runoff. Retention capacity was allowed to recover by evaporation during periods of no rainfall.

EXPLANATION

● Dubuque, Iowa -- Long-term recording rainfall site, see table 2.

D01 --- Map code for streamflow station, see table 3.

T01 --- Map code for streamflow station, see table 3.



The log-Pearson Type III distribution, fit by the method of moments, was used to quantify synthetic T-year flood estimates for each model/rain-gage application.

Formulation of Multiple-Regression Model

The rainfall-runoff model simulates a flood hydrograph and associated peak discharge rate by routing a volume of runoff (pattern of rainfall excess) with a model of an instantaneous unit hydrograph, *IUH*. With this two-phase operation as a guide, two factors were defined--an infiltration factor, *F*, and a hydrograph shape factor, *L*, that characterize the separate effects of model parameters on the volume of runoff and the shape of the *IUH*. Using these two factors as independent variables, a multiple-regression model was formulated to give a generalized definition of synthetic T-year floods (dependent variable) for each rainfall record, as follows,

$$\hat{q}_{i,j} = \alpha_i L_j^{b_{1i}} F_j^{b_{2i}}, \quad (2)$$

where

$\hat{q}_{i,j}$ = predicted value of standardized, synthetic discharge in cubic feet per second per square mile for the *i*-th recurrence interval, *i* = 2-, 25-, and 100-years, for the *j*-th model application, *j* = 1 to 50 (drainage area is a scalar multiplier in rainfall-runoff model computations; therefore, the results were "standardized" by dividing by the drainage area),

L_j = lag of *IUH*, see table 3,

F_j = infiltration factor, see table 3,

α_i = regression constant for *i*-th recurrence interval, and

b_{1i}, b_{2i} = regression coefficients for *i*-th recurrence interval.

Lag time has been successfully used as a hydrograph shape factor in observed flood-frequency studies by Carter (1961), Martens (1968), and Anderson (1970), and was selected for use in the analysis of synthetic flood-frequency characteristics. The lag, *L*, of the rainfall-runoff model routing component is the expected value of the distribution of arrival times of the ordinates of the *IUH*. According to Kraijenhoff van de Leur (1966), the lag of the rainfall-runoff model *IUH* is a linear combination of the

reservoir recession coefficient, KSW , and the time base, TC , of the isosceles translation hydrograph

$$L = KSW + 0.5TC, \quad (3)$$

where

L = lag of instantaneous unit-hydrograph, in hours,
 KSW = linear reservoir recession coefficient, in hours, and
 TC = time base of isosceles translation hydrograph, in hours.

An infiltration factor, F , was formulated to characterize the interactive effects of infiltration component parameters on the volume of storm runoff. The factor is defined as the infiltration capacity associated with an antecedent soil-moisture condition of 85 percent of field capacity, $BMS/BMSM = 0.85$, and accumulated storm infiltration of two inches, $SMS = 2$. These conditioning values of SMS and $BMS/BMSM$ were estimated by analysis of the value and sensitivity of the standard error of estimate for trial regressions using various combinations of these values. The form of infiltration equation used in rainfall-runoff model computations is

$$FR = KSAT[1.0 + (PSP/SMS) \cdot (RGF \cdot (1.0 - BMS/BMSM) + (BMS/BMSM))], \quad (4)$$

and substitution of the conditioning values of $SMS = 2$, and $BMS/BMSM = 0.85$, yields the formulation for F as

$$F = KSAT[1.0 + 0.5 \cdot PSP \cdot (0.15 RGF + 0.85)] \quad (5)$$

Regression Analysis of Synthetic T-Year Floods--Rural Model Applications

For each rainfall site, the synthetic T-year floods representative of the rural model applications (sample of 50) were related to rainfall-runoff model parameters by use of equation 2. The magnitude of the regression constants and coefficients will reflect the influence of climate as it is imbedded in the data used for synthesis. The rainfall-runoff model did not change from rainfall site to rainfall site, nor did the sample of model parameters. The only thing that influences the variability in output, from rainfall site to rainfall site, is the difference in input data--a reflection of climate.

The multiple-regression analyses show an increase in the accuracy of the relations with increasing recurrence interval, and also in a north-to-south direction (table 4). This is due to a decrease in the variability, and an increase in the average level of modeled antecedent soil-moisture associated with increasing recurrence interval, and with higher rainfall in the South. The regression model does not explicitly include the influence of the variability of the parameter $BMSM$, and to a certain degree, the affect of its variability on synthesis results is attenuated by high rainfall, both north-to-south and with increasing recurrence interval.

The regression coefficient, b_1 , which describes the influence of hydro-graph shape on T-year floods, shows low variability both geographically and with increasing recurrence interval. This is a reflection of the linearity of the rainfall-runoff model routing component--double the volume, double the peak. The regression constant, a , and coefficient, b_2 , show strong geographic variability, and are highly related as shown in figure 3. This empirical relationship indicates that the rainfall-runoff model is "well behaved" in the sense that it performs in a systematic manner when different rainfall records are used to synthesize annual floods. More importantly, the relationship suggests that the regression model could be modified by expressing the coefficient b_{2_i} a function of a_i , and thereby eliminate the need to define the geographic variability of b_{2_i} . That is,

$$b_{2_i} = f(a_i) = \gamma \log a_i + \beta, \tag{6}$$

where the parameters $\gamma = 0.41$, and $\beta = -1.39$, describe the line approximating the relationship indicated in figure 3. In addition, the low variability of the regression coefficient, b_{1_i} , (coefficient of variation = 0.13) suggests that it could be assigned its mean value, $\bar{b}_1 = -0.69$, with little loss of accuracy.

A second, "constrained" regression model was formulated as

$$\hat{q}_{i,j} = a_i \cdot L_j^{-0.69} \cdot F^{f(a_i)}, \tag{7}$$

and the single coefficient, a_i , was determined for each recurrence interval, to minimize the sum of the squares of the difference in the logarithms of

flow by a direct search procedure; that is, $Min \sum_{j=1}^{50} (\log \hat{q}_{i,j} - \log q_{i,j})^2$.

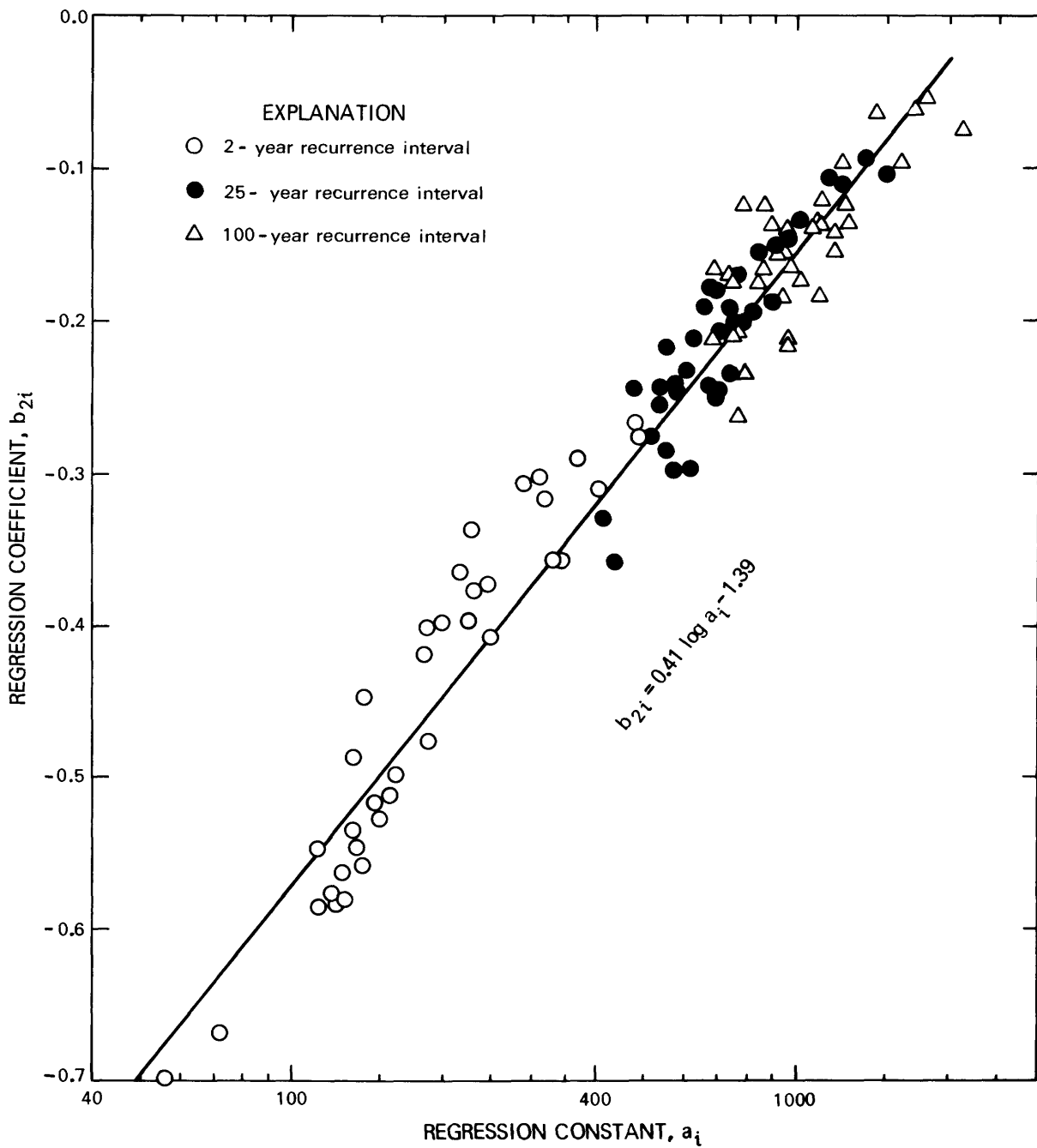


Figure 3.--Relation between regression constant, a_i , and regression coefficient, b_{2i} .

The results shown in table 5 indicate that the constrained, single-coefficient regression model is a reasonable substitute for the initial multiple-regression model, with only slightly higher standard errors of estimate and similar trends in the accuracy of the relations as a function of recurrence interval and geographic location.

Effects of Imperviousness on Synthetic Floods

The unit-hydrograph concept of linearity, that relates flow rate to volume of runoff (double the volume, double the peak), was used to formulate a model to quantify the effect of the increased volume of runoff from impervious areas on synthetic T-year floods. If we neglect the difference in the time patterns of rainfall excess generated from pervious and impervious contributing areas, then

$$\frac{P_I}{P} \sim \frac{V_I}{V} \sim \frac{V(1-I) + R \cdot I}{V}, \quad (8)$$

where

P_I = peak with impervious area contribution,

P = peak without impervious area contribution,

V_I = volume runoff with impervious area contribution,

V = volume runoff without impervious area contribution,

I = proportion of drainage area with impervious surface,

R = volume of storm rainfall.

The ratio on the right-hand side of the approximation is analogous to the "coefficient of imperviousness", K , introduced by Carter (1961) to describe the variability of floods from urban watersheds. By rearranging terms, then

$$P_I \sim P[1 + I \left(\frac{R}{V} - 1\right)]. \quad (9)$$

If we consider that the regression relation without impervious effects indicates that

$$P = aL^{-0.69} F^f(a), \quad (10)$$

and that

$$V \propto F_j^f(a), \quad (11)$$

and specify

$$d \propto R, \quad (12)$$

then a general regression relation for both rural and impervious area model applications may be defined as

$$\hat{q}_{i,j} = \alpha_{i,j} L_j^{-0.69} F_j^f(\alpha_i) [1.0 + I_j \left(\frac{d_i}{F_j^f(\alpha_i)} - 1.0 \right)]. \quad (13)$$

The unknown coefficient, d_i , can be determined by a least-squares fit, just as α_i was determined in the analysis of the rural model applications. That is,

$$\text{Min} \sum_{j=1}^{500} (\log \hat{q}_{i,j} - \log q_{i,j})^2, \quad (14)$$

by a direct search procedure. A summary of the results of the direct search determinations of the coefficient, d_i , is shown in table 6. The standard errors for the 2-year flood relations are consistently lower than those for rural-area model relations. This is because there is substantially less variability in the volumes of runoff and peak flow rates associated with the impervious-area model applications--there are minimum percentages of runoff (5, 10, 15, ...50 percent) from every storm event. Therefore, the adequacy of the infiltration factor, F , to characterize runoff volume is not as critical in the regression model formulation for impervious-area applications because there is a "platform" of runoff from every storm event.

Single-Coefficient Relation for Synthetic T-Year Floods

Similarly, as in the case of the initial rural-regression results, there is a strong relationship between the magnitudes of the regression parameters, in this case, α_i and d_i . This relationship, as shown in figure 4, indicates that two line segments are required to approximate the trend. Using these two approximating relations, equation 13 can be modified to yield a

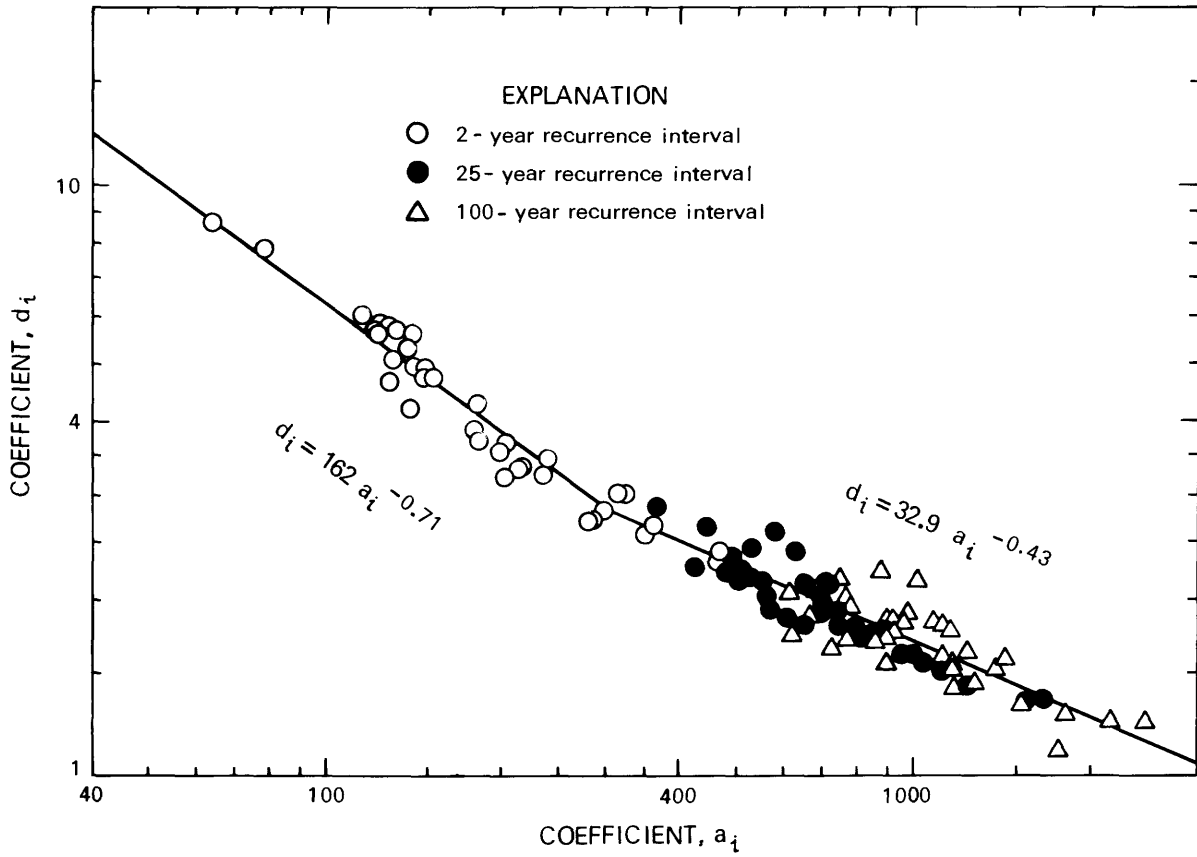


FIGURE 4. Relationship between the coefficients a_i , and d_i .

single-coefficient relation, a generalized definition, that describes both rural- and impervious-area model applications

$$\hat{q}_i = \alpha_i L_j^{-0.69} \frac{f(\alpha_i)}{F_j} \left[1.0 + I_j \left(\frac{g(\alpha_i)}{F_j f(\alpha_i)} - 1.0 \right) \right] \quad (15)$$

where

$$f(\alpha_i) = 0.41 \log \alpha_i - 1.39,$$

and

$$g(\alpha_i) = \begin{cases} 162 \alpha_i^{-0.71} & \text{for } \alpha_i \leq 300, \text{ and} \\ 32.9 \alpha_i^{-0.43} & \text{for } \alpha_i > 300. \end{cases}$$

The effectiveness of equation 15 to explain the variability of synthetic T-year floods is summarized in table 7. These results show that the generalized definition is a reasonably accurate relation that describes the results of synthesis for both rural- and impervious-area model applications. The average accuracy of the defining relation is somewhat better for the 25- and 100-year recurrence interval floods than that for 2-year floods, particularly in the North.

Geographic Variability of Climatic Factor, C

The site-to-site variability in the magnitude of the regression coefficient, α_i , in equation 15, is interpreted as reflecting the spatially varying influence of local climatic factors, C_i , on synthetic flood potential. Contour maps depicting the geographic variability of the climatic factor, C_i , that is, α_i , are shown in figures 5, 6, and 7. Estimates of the climatic factor, used in conjunction with the generalized definition of synthetic flood potential, equation 15, offer a means of integrating long-term rainfall information into a procedure to improve T-year flood estimates at rainfall-runoff model calibration sites. The remainder of this report develops and evaluates such a procedure.

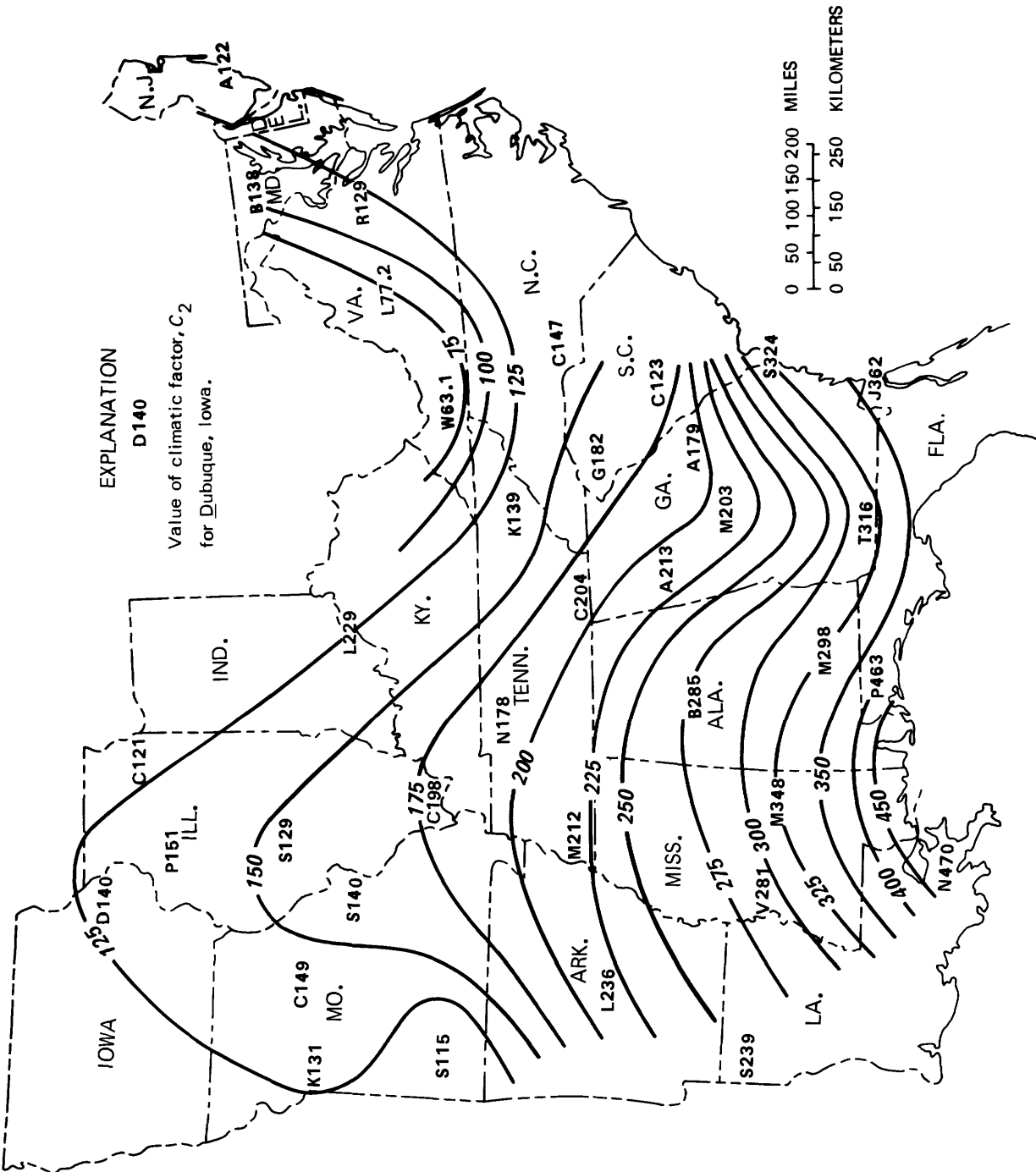


FIGURE 5.— Contour map showing the geographic variation in the 2-year recurrence interval climatic factor, C_2 .

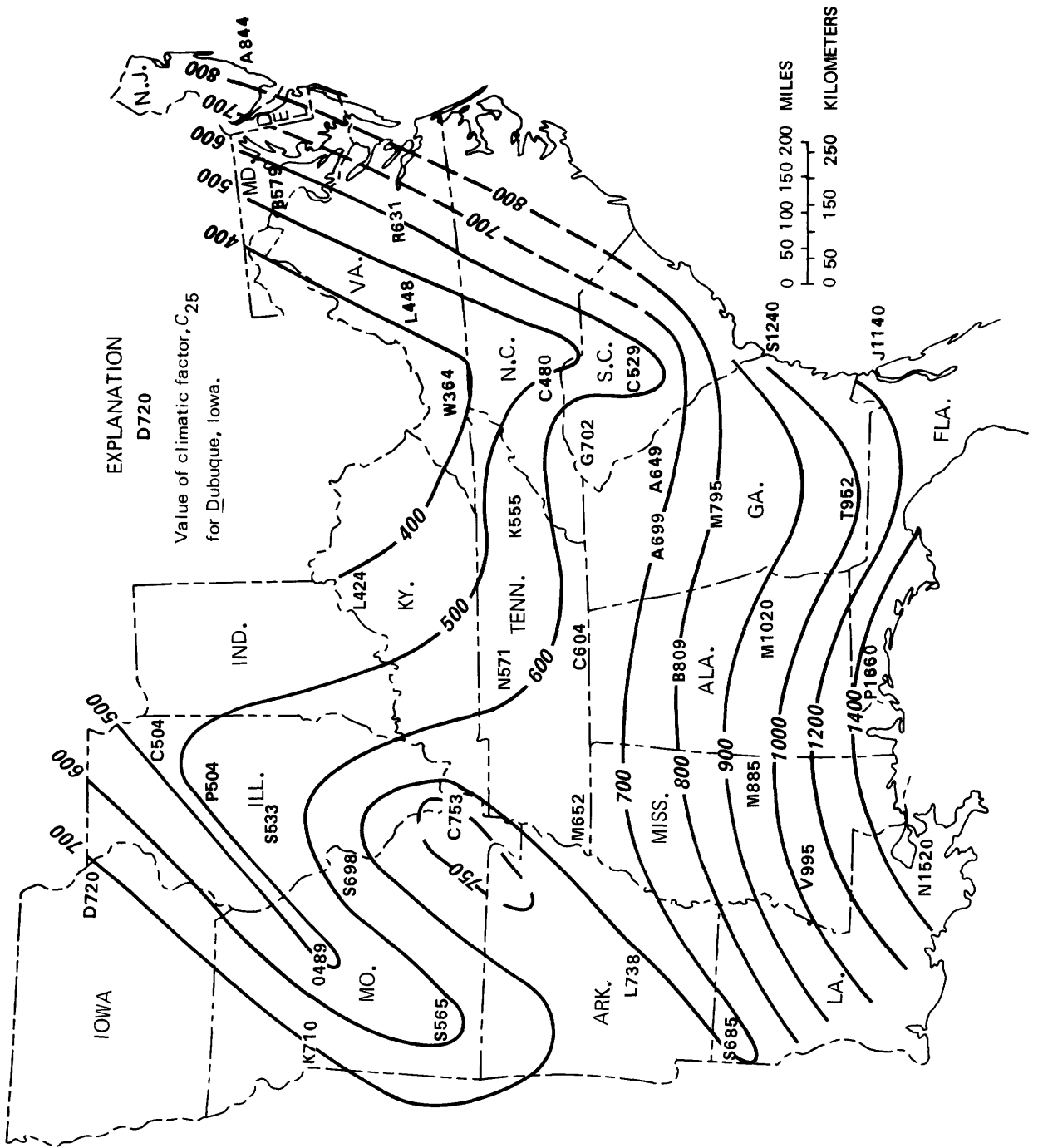


FIGURE 6. --- Contour map showing the geographic variation in the 25-year recurrence interval climatic factor, C_{25} .

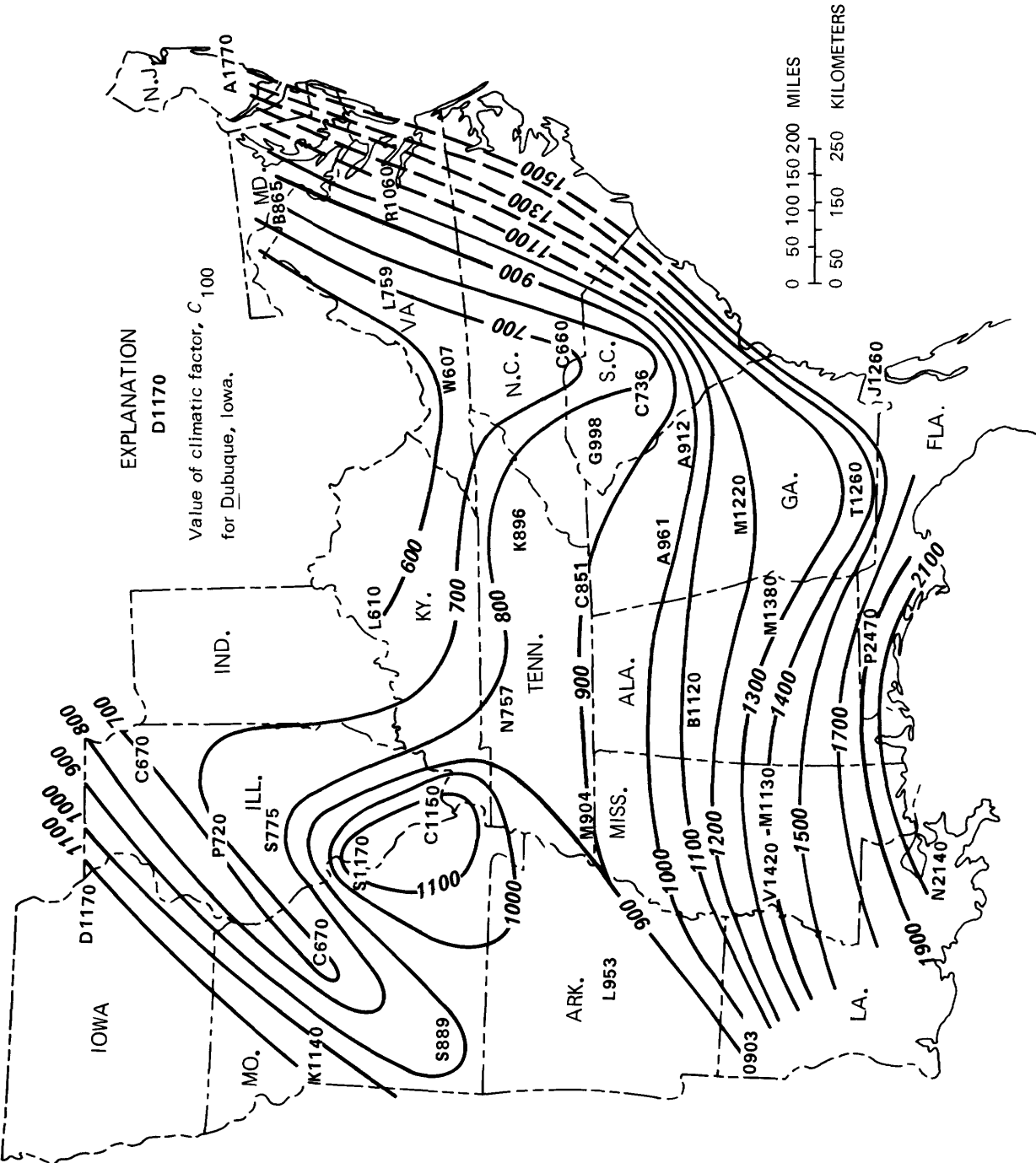


FIGURE 7. — Contour map showing the geographic variation in the 100—year recurrence interval climatic factor, C_{100} .

MAP-MODEL ESTIMATES OF T-YEAR FLOODS AT CALIBRATION SITES

Map-model estimates of the 2-, 25-, and 100-year recurrence interval floods can be computed for rainfall-runoff model calibration sites as follows:

1. Determine values of the climatic factors, C_2 , C_{25} , and C_{100} for the site location using figures 5, 6, and 7.
2. Compute model lag, L , using equation 3.
3. Compute the infiltration factor, F , using equation 5.
4. Compute the standardized discharge as,

$$\hat{q}_i = C_i^L \frac{-0.69 f(C_i)}{F} \left[1.0 + I\left(\frac{g(C_i)}{f(C_i)} - 1.0\right) \right], \quad (16)$$

where

$$f(C_i) = 0.41 \log C_i - 1.39,$$

$$g(C_i) = \begin{cases} 162C_i^{-0.71} & C_i \leq 300, \text{ and} \\ 32.9C_i^{-0.43} & C_i > 300. \end{cases}$$

5. Compute map-model estimates of the T-year floods as,

$$\hat{Q}_i = A\hat{q}_i, \quad (17)$$

where

A = drainage area in square miles.

If it is assumed that the log-Pearson Type III distribution is the underlying population defining the frequency of map-model flood estimates, then estimates of the distribution parameters, that is, estimates of the mean, \bar{X} , the standard deviation, S , and the skew coefficient, G , can be computed by using the values for the 2-, 25-, and 100-year flood magnitudes, and table

look-up procedures involving percentage points of the distribution as tabulated by Harter (1969), as follows:

1. Use the values for \hat{Q}_2 , \hat{Q}_{25} , and \hat{Q}_{100} as previously determined, to compute the factor R , using

$$R = \frac{(\log \hat{Q}_{25} - \log \hat{Q}_2)}{(\log \hat{Q}_{100} - \log \hat{Q}_2)}, \quad (18)$$

and determine the skew coefficient, G , from the following table relating R and G .

G	R	G	R	G	R	G	R	G	R	G	R
-3.0	0.99712	-2.0	0.95495	-1.0	0.84377	0.0	0.75255	1.0	0.69250	2.0	0.64563
-2.9	.99590	-1.9	.94582	-0.9	.83279	.1	.74547	1.1	.68745	2.1	.64120
-2.8	.99431	-1.8	.93585	-.8	.82222	.2	.73870	1.2	.68252	2.2	.63678
-2.7	.99220	-1.7	.92516	-.7	.81206	.3	.73220	1.3	.67768	2.3	.63236
-2.6	.98946	-1.6	.91392	-.6	.80235	.4	.72594	1.4	.67293	2.4	.62794
-2.5	.98600	-1.5	.90229	-.5	.79306	.5	.71991	1.5	.66825	2.5	.62352
-2.4	.98170	-1.4	.89044	-.4	.78419	.6	.71408	1.6	.66364	2.6	.61908
-2.3	.97651	-1.3	.87853	-.3	.77573	.7	.70844	1.7	.65908	2.7	.61464
-2.2	.97032	-1.2	.86672	-.2	.76766	.8	.70298	1.8	.65457	2.8	.61017
-2.1	.96351	-1.1	.85509	-.1	.75993	.9	.69767	1.9	.65009	2.9	.60568
										3.0	.60117

The above table may be extended using the relation

$$R = \frac{(K_{25} - K_2)}{(K_{100} - K_2)}, \quad (19)$$

where K_i is the Pearson Type III deviate (Water Resources Council, 1976, appendix 3.)

2. Compute the standard deviation, S , using

$$S = \frac{\log(\hat{Q}_{25}/\hat{Q}_2)}{DK} \quad (20)$$

where DK is determined as a function of skew coefficient, G , from the following table.

G	DK	G	DK	G	DK	G	DK	G	DK	G	DK
-3.0	0.27031	-2.0	0.65233	-1.0	1.20187	0.0	1.75069	1.0	2.20666	2.0	2.52573
-2.9	.29845	-1.9	.70229	-.9	1.25913	.1	1.80124	1.1	2.24541	2.1	2.54858
-2.8	.32874	-1.8	.75393	-.8	1.31614	.2	1.85081	1.2	2.28275	2.2	2.56966
-2.7	.36125	-1.7	.80705	-.7	1.37274	.3	1.89942	1.3	2.31863	2.3	2.58894
-2.6	.39604	-1.6	.86144	-.6	1.42885	.4	1.94690	1.4	2.35303	2.4	2.60643
-2.5	.43314	-1.5	.91686	-.5	1.48438	.5	1.99324	1.5	2.38587	2.5	2.62209
-2.4	.47253	-1.4	.97307	-.4	1.53923	.6	2.03841	1.6	2.41715	2.6	2.63595
-2.3	.51423	-1.3	1.02988	-.3	1.59336	.7	2.08238	1.7	2.44681	2.7	2.64800
-2.2	.55815	-1.2	1.08708	-.2	1.64674	.8	2.12510	1.8	2.47482	2.8	2.65823
-2.1	.60423	-1.1	1.14446	-.1	1.69918	.9	2.16655	1.9	2.50113	2.9	2.66667
										3.0	2.67334

The above table may be extended using the relation

$$DK = (K_{25} - K_2). \quad (21)$$

3. Compute the mean, \bar{X} , using,

$$\bar{X} = \log (\hat{Q}_2) - K_2 S \quad (22)$$

where K_2 is a function of skew, G , as shown below.

G	K ₂	G	K ₂	G	K ₂	G	K ₂	G	K ₂	G	K ₂
-3.0	0.39554	-2.0	0.30685	-1.0	0.16397	0.0	0.00000	1.0	-0.16397	2.0	-0.30685
-2.9	.38991	-1.9	.29443	-0.9	.14807	.1	-.01662	1.1	-.17968	2.1	-.31872
-2.8	.38353	-1.8	.28150	-.8	.13199	.2	-.03325	1.2	-.19517	2.2	-.32999
-2.7	.37640	-1.7	.26808	-.7	.11578	.3	-.04993	1.3	-.21040	2.3	-.34063
-2.6	.36852	-1.6	.25422	-.6	.09945	.4	-.06651	1.4	-.22535	2.4	-.35062
-2.5	.35992	-1.5	.23996	-.5	.08302	.5	-.08302	1.5	-.23996	2.5	-.35992
-2.4	.35062	-1.4	.22535	-.4	.06651	.6	-.09945	1.6	-.25422	2.6	-.36852
-2.3	.34063	-1.3	.21040	-.3	.04993	.7	-.11578	1.7	-.26808	2.7	-.37640
-2.2	.32999	-1.2	.19517	-.2	.03325	.8	-.13199	1.8	-.28150	2.8	-.38353
-2.1	.31872	-1.1	.17968	-.1	.01662	.9	-.14807	1.9	-.29443	2.9	-.38991
										3.0	-.39554

Using these values for the mean, standard deviation, and skew, additional map-model T-year flood estimates can be computed for any desired recurrence interval using the relation

$$\hat{Q}_T = \text{antilog} (\bar{X} + K_T S). \quad (23)$$

Comparison of Observed and Map-Model Flood Estimates

Observed and map-model estimates of T-year floods were computed for 98 rainfall-runoff model calibration sites shown in figure 2, and summarized in table 3. The sample includes 49 of the 50 basins initially selected for use in developing the synthetic flood relations, plus an additional selection of 49 sites to add "strength in numbers"; thus, it was hoped to yield a more meaningful sample for use in comparing observed and map-model flood estimates. Observed T-year flood estimates, Q_i , were computed using procedures recommended by the Water Resources Council (1976). Map-model flood estimates, \hat{Q}_i , and associated log-Pearson Type III distribution statistics, \bar{X} , S , and G were computed using the methods previously outlined.

Scatter diagrams of observed, \tilde{Q}_i , versus map-model, \hat{Q}_i , flood estimates are shown in figure 8. The plots indicate that map-model estimates of the 25- and 100-year floods are generally lower than observed estimates. A comparison of the average values of distribution statistics and T-year floods, in \log_{10} units, is shown below.

Average	Observed	Map-model
\bar{X}	2.497	2.499
S	0.298	0.264
G	-0.109	-0.261
$\log_{10} Q_2$	2.502	2.512
$\log_{10} Q_{25}$	3.004	2.929
$\log_{10} Q_{100}$	3.161	3.049

If it is assumed that on the average, the observed estimates comprise an unbiased time-sample, that is, for each recurrence interval

$$\frac{1}{98} \sum_{j=1}^{98} \hat{Q}_j = \frac{1}{98} \sum_{j=1}^{98} \text{True } Q_j, \quad (24)$$

then the map-model estimates are apparently biased and should be adjusted to remove the discrepancy in average values shown above. Thus, the generalized definition was modified such that

$$\text{"unbiased" } \hat{q}_i = B_i \hat{Q}_i, \quad (25)$$

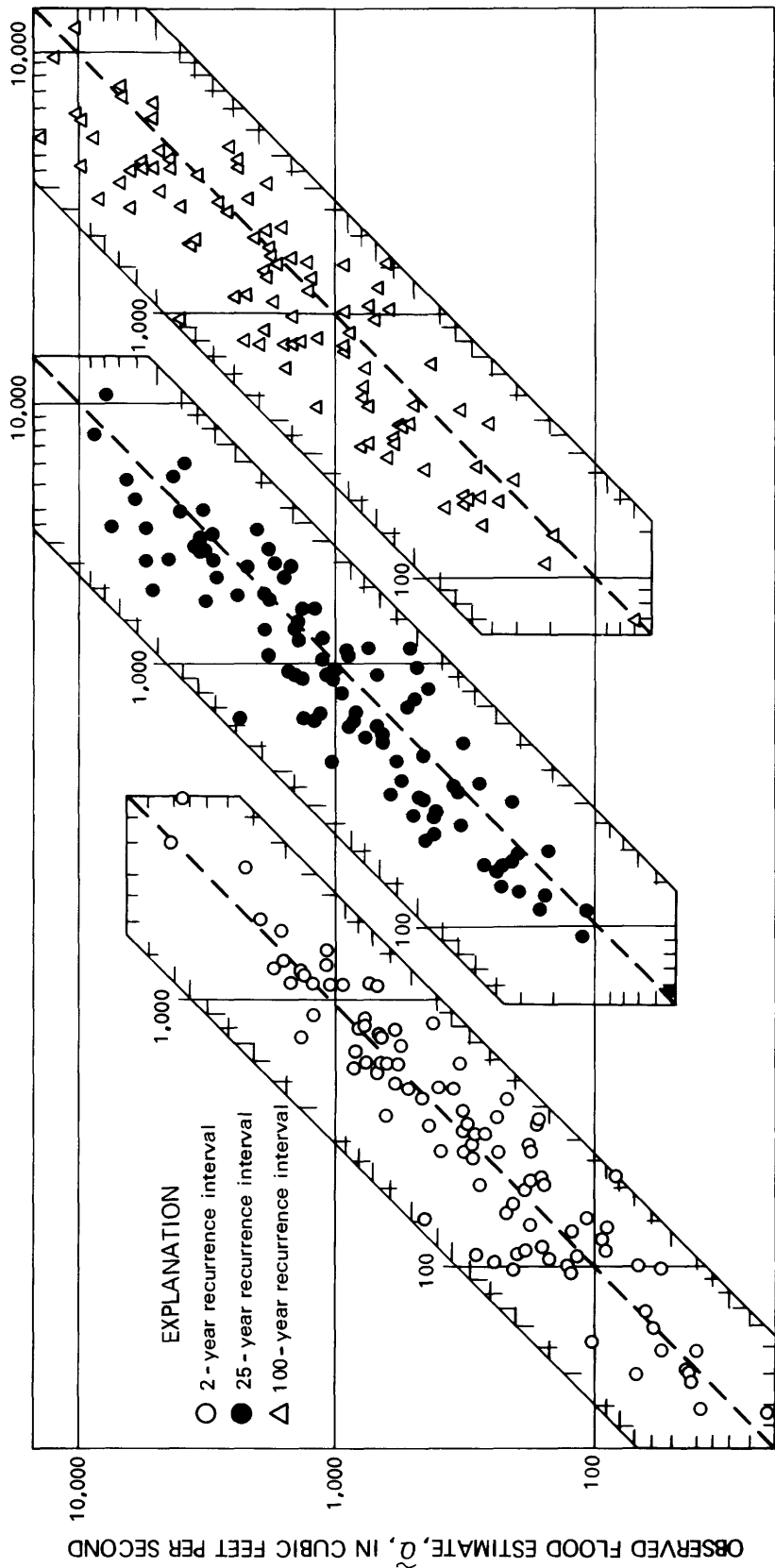


FIGURE 8.-- Scatter diagrams of observed and map-model T-year flood estimates.

where

B_i = the average map-model bias, $B_2 = 0.98$, $B_{25} = 1.19$, and $B_{100} = 1.29$.

ACCURACY AND WEIGHTING OF OBSERVED AND MAP-MODEL T-YEAR FLOODS

We have two essentially independent estimates: the map-model estimate $\hat{Q}_{i,j}$, and the observed estimate $\tilde{Q}_{i,j}$, of the true but unknown T-year flood $Q_{i,j}$. We seek to appraise the accuracy, in some average sense, of the map-model estimating procedure, equation 25, and to develop a method of weighting observed and map-model T-year flood estimates. The logarithmic transform of the map-model estimate of the true flood can be written as

$$\log \hat{Q}_{i,j} = \log Q_{i,j} + \alpha_{i,j}, \quad (26)$$

where $\alpha_{i,j}$ reflects a lumping of error terms including:

- (1) error in the rainfall-runoff model (infiltration, routing, etc.),
- (2) error in the calibrated model parameters (*KSW*, *KSAT*, etc.),
- (3) error in the generalized synthetic flood relation, equation 15,
- (4) error in the maps depicting the influence of climate, C_i , on synthetic T-year floods, including resolution, time-sampling, and measurement errors, and
- (5) error in determination and applicability of the average bias coefficients, B_i , equation 25.

If we assume that the expected value of $\alpha_{i,j}$ has mean zero, that is, $\log \hat{Q}_{i,j}$ is unbiased, then the variance of $\alpha_{i,j}$ is

$$\text{Var}[\alpha_{i,j}] = E[(\log \hat{Q}_{i,j} - \log Q_{i,j})^2]. \quad (27)$$

Similarly, the logarithmic transform of the observed estimate of the true flood is given by

$$\log \tilde{Q}_{i,j} = \log Q_{i,j} + \epsilon_{i,j}. \quad (28)$$

If we ignore errors in measurement of discharge and errors in assumptions of the underlying population distribution, then the error term $\varepsilon_{i,j}$, is solely a function of record length, that is, time-sampling error. If we assume that the expected value of $\varepsilon_{i,j}$ has mean zero, that is, $\hat{Q}_{i,j}$ is unbiased, then the variance of $\varepsilon_{i,j}$ is

$$\text{Var}[\varepsilon_{i,j}] = E[(\log \tilde{Q}_{i,j} - \log Q_{i,j})^2]. \quad (29)$$

Although both the variance of $\alpha_{i,j}$ and $\varepsilon_{i,j}$ may vary from site-to-site, we seek an overall, average measure of the error variance of the map-model estimating procedure, such as

$$\overline{\text{Var}}[\alpha_i] = \frac{1}{M} \sum_{j=1}^M E[(\log \hat{Q}_{i,j} - \log Q_{i,j})^2]; \quad (30)$$

in terms of an overall, average measure of the time-sampling error variance of the observed flood estimates, such as

$$\overline{\text{Var}}[\varepsilon_i] = \frac{1}{M} \sum_{j=1}^M E[(\log \tilde{Q}_{i,j} - \log Q_{i,j})^2]. \quad (31)$$

A similar average measure of adequacy is found in regression analysis, where the standard error of estimate is taken as a measure of accuracy of regression estimates, even though the variance of any individual estimate is not constant for all values of the independent variables.

One method of obtaining an estimate of $\overline{\text{Var}}[\alpha_i]$ is as follows. The squared differences in $\log \hat{Q}_{i,j}$, and $\log \tilde{Q}_{i,j}$ can be written as

$$\begin{aligned}
(\log \hat{Q}_{i,j} - \log \tilde{Q}_{i,j})^2 &= (\log \hat{Q}_{i,j} - \log Q_{i,j} + \log Q_{i,j} - \log \tilde{Q}_{i,j})^2, \\
&= (\log \hat{Q}_{i,j} - \log Q_{i,j})^2 + (\log \tilde{Q}_{i,j} - \log Q_{i,j})^2 \\
&\quad - 2(\log \hat{Q}_{i,j} - \log Q_{i,j})(\log \tilde{Q}_{i,j} - \log Q_{i,j}). \quad (32)
\end{aligned}$$

If the deviations $(\log \hat{Q}_{i,j} - \log Q_{i,j})$ and $(\log \tilde{Q}_{i,j} - \log Q_{i,j})$ are considered independent in a statistical sense, then by taking expectations and rearranging terms

$$\begin{aligned}
E[(\log \hat{Q}_{i,j} - \log Q_{i,j})^2] &= E[(\log \hat{Q}_{i,j} - \log \tilde{Q}_{i,j})^2] - \\
&\quad E[(\log \tilde{Q}_{i,j} - \log Q_{i,j})^2], \quad (33)
\end{aligned}$$

or

$$\text{Var}[\alpha_{i,j}] = \text{Var}[n_{i,j}] - \text{Var}[\varepsilon_{i,j}], \quad (34)$$

where

$$\text{Var}[n_{i,j}] = E[(\log \hat{Q}_{i,j} - \log \tilde{Q}_{i,j})^2]. \quad (35)$$

According to Hardison (1971), $\text{Var}[\varepsilon_{i,j}]$ can be estimated by $R^2_{i,j} S^2_j / N_j$, that is,

$$\hat{\text{Var}}[\varepsilon_{i,j}] = R^2_{i,j} S^2_j / N_j, \quad (36)$$

where $R^2_{i,j}$ is a function of recurrence interval and skew coefficient (Hardison, 1971, table 2), S^2_j is the sample estimate of the variance of the

logarithms of observed annual peaks, and N_j is the number of observed annual peaks. The quantities $Var[n_{i,j}]$ can be directly estimated because both $\hat{Q}_{i,j}$ and $\tilde{Q}_{i,j}$ are available. Thus, averaging over all sites gives an estimate of the average map-model error variance, $\overline{Var}[\alpha_i]$ as

$$\overline{VMM}_i = \overline{SD}_i - \overline{VT}_i, \quad (37)$$

where

$$\overline{SD}_i = \frac{1}{M-1} \sum_{j=1}^M (\log \hat{Q}_{i,j} - \log \tilde{Q}_{i,j})^2, \quad (38)$$

and

$$\overline{VT}_i = \frac{1}{M} \sum_{j=1}^M R_{i,j}^2 S_j^2 / N_j. \quad (39)$$

The averaging factor, $M-1$, used in the computation of the mean squared logarithmic deviation, \overline{SD}_i , accounts for a lost degree of freedom associated with the determination of the average bias coefficients, B_i . A word of caution is necessary when using this method of decomposing variance components. Because \overline{SD}_i and \overline{VT}_i are computed independently of one another, negative values of \overline{VMM}_i may result, which are not meaningful.

The preceding formulaton is similar to that developed by Hardison, (1971, equation 3), in his study of prediction error of regression estimates of streamflow characteristics:

$$V_S = V_R - (1 - \rho)\overline{V}_T, \quad (40)$$

where

V_S = variance due to space-sampling error; same as model error,

V_R = variance of the regression, the square of the standard error of estimate of a regression,

ρ = average interstation correlation coefficient, and

\overline{V}_T = average variance of the time-sampling error at the stations used in the regression.

The analogy between the two formulations is as follows: \overline{VMM} is analogous to V_S , \overline{SD} is analogous to V_R and \overline{VT} is analogous to $\overline{V_T}$. The influence of the average interstation correlation, ρ , is not accounted for in equation 37, but its absence is thought to be of minor importance in the present analysis ($\rho = 0.06$ for the 98-station sample).

If it is assumed that the two estimates $\hat{Q}_{i,j}$, and $\tilde{Q}_{i,j}$, are independent and unbiased, then a weighted estimate, $WQ_{i,j}$, can be formed as

$$WQ_{i,j} = WMM_{i,j} \cdot \hat{Q}_{i,j} + WO_{i,j} \cdot \tilde{Q}_{i,j}, \quad (41)$$

where the map-model weighting factor is

$$WMM_{i,j} = \frac{R^2_{i,j} S^2_{j/N_j}}{(R^2_{i,j} S^2_{j/N_j} + \overline{VMM}_i)}, \quad (42)$$

and the observed weighting factor is

$$WO_{i,j} = 1 - WMM_{i,j}. \quad (43)$$

The variance of the weighted estimate is less than the variance of either the map-model or the observed estimate, and is given by

$$VW_{i,j} = \frac{\overline{VMM}_i \cdot R^2_{i,j} S^2_{j/N_j}}{(\overline{VMM}_i + R^2_{i,j} S^2_{j/N_j})}. \quad (44)$$

The average value of the error variance of the weighted estimates may be expressed as

$$\overline{VW}_i = \frac{1}{M} \sum_{j=1}^M VW_{i,j}. \quad (45)$$

Equations 37, 38, 39, and 45 were used to compute estimates of the average values of the map-model error variance, \overline{VMM}_i , the time-sampling variance, \overline{VT}_i , and the error variance of the weighted estimates, \overline{VW}_i , using observed and map-model flood data for the test sample of 98 rural-area calibration sites. The trends in the values of these variance components are shown as a function of recurrence interval in figure 9. The rapid decrease in the magnitude of the average map-model error variance, from the 1.25-year to the 5-year recurrence interval, is a reflection of the accuracy of the synthetic T-year flood relation, as a function of recurrence interval, and the general accuracy characteristics of the rainfall-runoff model in the reproduction of small-magnitude floods.

The synthetic T-year flood relation is less accurate at low recurrence intervals because of the absence of the parameter, $BMSM$, and because the influence of modeled antecedent soil-moisture conditions, BMS , and SMS , are not explicitly included, nor can they be explicitly included, in the defining relation. SMS and BMS are model variables, not model parameters, and their influence on synthesis results can only be approximated in an average sense, that is, by the "conditioning" values, as previously determined. Modeled antecedent conditions, the influence of $BMSM$, and the adequacy of the infiltration factor, F , are less important in explaining synthetic results for the higher recurrence interval floods, because they are attenuated.

Similarly, the influence of real-world, antecedent soil-moisture conditions are only approximately modeled by the rainfall-runoff model; they are very important in explaining the variability of flood magnitudes from lower magnitude storms, and resulting generally lower magnitude floods. The rainfall-runoff model is more accurate in reproducing extreme floods than minor ones. Extreme floods from small basins are extreme for several reasons, but high rainfall intensity/duration dominates. In general, infiltration losses become a less significant part of total rainfall for extreme rainfall events--a threshold effect. The inadequacies in modeled soil-moisture conditions and in the infiltration component tend to be attenuated for the larger events. Storm rainfall assumes a dominant role in determining the output, both in nature and in the rainfall-runoff model abstraction of it, as well as in the regression model abstraction of rainfall-runoff model.

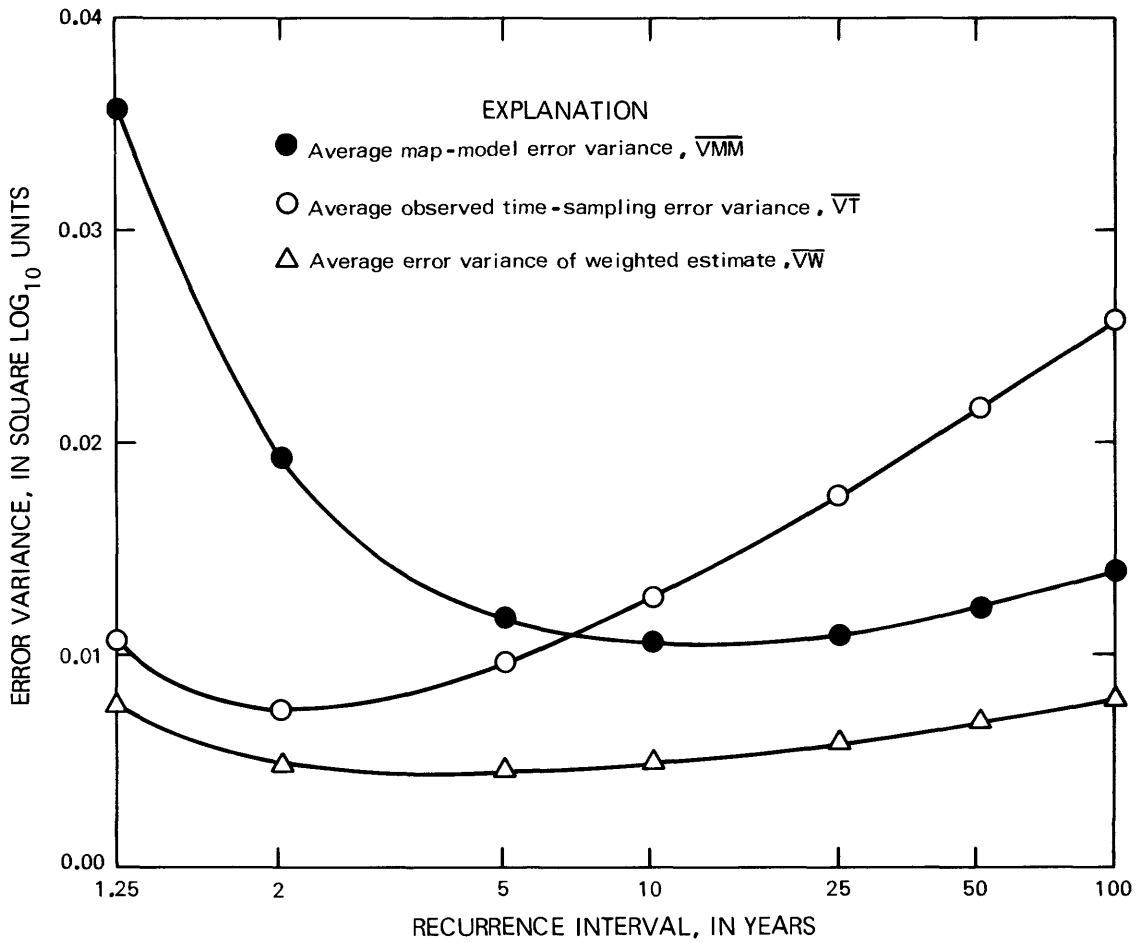


FIGURE 9. -- Trends in error-variance components as a function of recurrence interval.

The average map-model error variance decreases to a minimum value of about 0.011 squared log units at the 10-year recurrence interval; then reverses its trend and increases with increasing recurrence interval--a desirable outcome. Without this reversal, the ascribed value of the map-model estimating procedure, in terms of the concept of equivalent-year accuracy (Carter and Benson, 1970), would increase without limit. Logic tells us that there is an upper limit to the amount of information that can be extracted from long-term rainfall records, in this case about 65 years, because that is the average length of record used in the development of the map-model estimating procedure. Obviously, this is an unattainable upper limit, because of the many sources of error inherent in the map-model estimating procedure, including errors in the rainfall-runoff model, the generalized definitions, and the maps depicting the geographic variability of the inferred effect of climate on synthetic floods.

The trend in the average time-sampling error variance of the observed T-year flood estimates, with a minimum near the 2-year recurrence interval, is a completely predictable statistical outcome. This is because the 2-year flood is less affected by time-sampling error than are the flood levels associated with the tails of the distribution, where the error in sample estimates of the standard deviation and skew coefficient is more influential.

The average error variance of the weighted flood estimates, \overline{VW}_i , shows the worth of the map-model estimating procedure in relation to observed data estimates that have a harmonic-mean record length of 13.2 years. Note particularly the "flatness" in the trend of \overline{VW}_i as a function of recurrence interval, and that the average accuracy of the weighted estimates of the 100-year floods is equivalent to that of the observed data estimates of the 2-year floods. The average accuracy of the weighted T-year flood estimates can be appraised in terms of equivalent-length of observed record using the relation

$$NE_i = NG \frac{\overline{VT}_i}{\overline{VW}_i} \quad (46)$$

where

NE_i = average equivalent record length of weighted estimates, in years,

NG = harmonic-mean record length of observed annual flood records
(13.2 years).

The following table shows estimates of the equivalent record lengths of the weighted flood estimates at selected recurrence intervals.

Recurrence interval (years)	Equivalent record length (years)
1.25	19
2	20
5	28
10	34
25	40
50	43
100	44

These results show a pronounced nonlinearity in equivalent record length as a function of recurrence interval, and also indicate an upper limit to the amount of peak-flow information attainable by the map-model estimating procedure--a gain of about 30 years of record for estimating the higher recurrence interval floods (the 50- and 100-year floods), as compared to a gain of about 6 years of record for estimating the lower recurrence interval floods (the 1.25- and 2-year floods).

SUMMARY AND CONCLUSIONS

Annual flood series were synthesized for a wide variety of modeled, hydrologic conditions using data from each of 36 long-term recording rainfall sites. A single-coefficient regression relation was developed for each rainfall site to give a generalized definition of synthetic T-year floods as a function of the rainfall-runoff model parameters. The accuracy of the generalized definition increases with an increase in recurrence interval, with an increase in percent impervious area, and in a north-to-south direction. These trends in accuracy are a ramification of the decreasing influence of the variability in infiltration component parameters (*KSAT*, *PSP*, *RGF*, and *BMSM*) on the increased volumes of runoff and peak discharge rates associated with increasing recurrence interval, increasing impervious area, and also with higher rainfall in the South. The extreme floods are extreme for several reasons, but high rainfall intensity/duration is a necessary condition. For the extreme events, modeled infiltration losses become a less significant part of total rainfall, and the effect of the site-to-site variability in infiltration component parameters is attenuated, as it should be. The site-to-site variability in the routing component parameters, those parameters that define the hydrograph shape factor *L*, assume a dominant role in explaining the reduced variability of extreme flood events. A general maxim for modeling the results of synthesis is "...the higher the variability, the more model data input required to explain the variability." The degree of variability, and thus the ability of the generalized definition to explain that variability, is inversely related to the magnitude of the flood event--it takes less model to explain the reduced variability in extreme floods, and more model to explain the higher variability in small magnitude events.

The site-to-site variability in the magnitude of the regression coefficient, α , that characterizes the generalized T-year flood relation, is a reflection of the spatially varying influence of climate, C , on the results of synthesis. Maps depicting the geographic variation in the magnitude of C were prepared and used in conjunction with fitted rainfall-runoff model parameters and the generalized synthetic flood relation to develop map-model, T-year flood estimates for 98 small-basin calibration sites. Comparisons of these T-year flood estimates with those based on observed annual floods show that the map-model estimating procedure is biased--the map-model estimates are generally lower than the observed estimates for return periods greater than the 2-year recurrence interval. This tendency for underestimation of the higher recurrence interval events may be attributed to several factors, including:

1. A loss of variance associated with a model smoothing effect, as described by Matalas and Jacobs (1964), and Kirby (1975);
2. The effect of unmodeled, real-world nonlinearities in the transformation of rainfall excess to discharge hydrograph (routing)--a limitation of the unit-hydrograph concept as used in the rainfall-runoff model;
3. Incorrectly modeled nonlinearities in the synthesis of rainfall excess (volume of runoff), due to inadequacies in either antecedent soil-moisture accounting or infiltration computations;
4. Sampling errors in the long-term rainfall data used for synthesis of annual floods;
5. The use of an average daily pattern of potential evapotranspiration.

Regardless of the particular cause or causes for the tendency to underestimate the higher recurrence interval floods, the bias can be removed in an average sense by using an average adjustment factor, that is, the bias coefficients, B_i .

The average accuracy of unbiased, map-model flood estimates was appraised for the sample of 98 rural-area calibration sites located in a six-state study area. This appraisal shows that the accuracy of the estimates increases rapidly, with increasing recurrence interval up to about the 10-year return period, and then reverses its trend and decreases slowly. This pattern of error variance, when compared to that associated with observed flood estimates, indicates that the map-model estimates are more accurate than the observed estimates beyond the 10-year recurrence interval (the harmonic-mean record length of the observed annual flood series is 13.2 years).

Improved T-year flood estimates were developed by computing a weighted average of observed and map-model estimates, and the accuracy of the improved estimates was appraised as a function of recurrence interval and in terms of the concept of equivalent-length of record. The trend in the accuracy of the improved estimates shows that the map-model estimating procedure yields an equivalent-length of observed record that ranges from a low of about 6 years for the 1.25-year flood, up to an ultimate, maximum level of about 30 years of data for estimating the 50- and 100-year recurrence interval floods.

REFERENCES

- Anderson, D. G., 1970, Effects of urban development on floods in Northern Virginia: U.S. Geological Survey Water-Supply Paper 2001-C, 22 p.
- Benson, M. A., 1962, Factors influencing the occurrence of floods in a humid region of diverse terrain: U.S. Geological Survey Water-Supply Paper 1580-B, 64 p.
- _____, 1964, Factors affecting the occurrence of floods in the Southwest: U.S. Geological Survey Water-Supply Paper 1580-D, 72 p.
- Carrigan, P. H., Jr., 1973, Calibration of U.S. Geological Survey rainfall-runoff model for peak flow synthesis--natural basins: U.S. Geological Survey Computer Contribution, 114 p. Available only from U.S. Department of Commerce, National Technical Information Service (NTIS), Springfield, Va. 22151, accession no. PB-226-217.
- Carter, R. W., 1961, Magnitude and frequency of floods in suburban areas, *in* Short papers in the geological and hydrologic sciences: U.S. Geological Survey Professional Paper 424-B, p. B9-B14.
- Carter, R. W., and Benson, M. A., 1970, Concepts for the design of streamflow data programs: U.S. Geological Survey Open-File Report, 33 p.
- Clark, C. O., 1945, Storage and the unit hydrograph: American Society of Civil Engineers Transactions, v. 110, p. 1419-1488.
- Colson, B. E., and Hudson, J. W., 1976, Flood frequency of Mississippi streams: U.S. Geological Survey Open-File Report, 34 p.
- Curtis, G. W., 1977, Frequency analysis of Illinois floods using observed and synthetic streamflow records: U.S. Geological Survey Water-Resources Investigations 77-104, 32 p.
- Dawdy, D. R., Lichty, R. W., and Bergmann, J. M., 1972, A rainfall-runoff model for estimation of flood peaks for small drainage basins: U.S. Geological Survey Professional Paper 506-B, 28 p.
- Golden, H. G., and Price, M., 1976, Flood-frequency analysis for small natural streams in Georgia: U.S. Geological Survey Open-File Report 76-511, 77 p.
- Hardison, C. H., 1971, Prediction error of regression estimates of streamflow characteristics at ungaged sites: U.S. Geological Survey Professional Paper 750-C, p. C228-C236.
- Harter, H. L., 1969, A new table of percentage points of the Pearson Type III distribution: Technometrics, v. 11, no. 1, p. 117-187.
- Hauth, L. D., 1974, Model synthesis in frequency analysis of Missouri floods: U.S. Geological Survey Circular 708, 16 p.
- Kirby, W., 1975, Model smoothing effect diminishes simulated flood peak variances (abs): American Geophysical Union Transactions, v. 56, no. 6, p. 361.
- Kraijenhoff van de Leur, D. A., 1966, Runoff models with linear elements: *in* Committee for Hydrological Research T.N.O., Recent trends in hydrograph synthesis: Verslagen En Mededelingen, Commissie Voor Hydrologisch Onderzoek T.N.O. 13, The Hague, p. 31-62.
- Martens, L. A., 1968, Flood inundation and effects of urbanization in metropolitan Charlotte, North Carolina: U.S. Geological Survey Water-Supply Paper 1591-C, 60 p.
- Matalas, N. C., and Jacobs, B., 1964, A correlation procedure for augmenting hydrologic data: U.S. Geological Survey Professional Paper 434-E, 7 p.

- McCain, J. F., 1974, Progress report on flood-frequency synthesis for small streams in Alabama: Alabama Highway Research, HPR70, 109 p.
- Philip, J. R., 1954, An infiltration equation with physical significance: Soil Science Society of America Proceedings, v. 77, p. 153-157.
- Thomas, D. M., and Benson, M. A., 1970, Generalization of streamflow characteristics from drainage-basin characteristics: U.S. Geological Survey Water-Supply Paper 1975, 55 p.
- Water Resources Council, 1976, Guidelines for determining flood-flow frequency: U.S. Water Resources Council Bulletin 17, 26 p.
- Wibben, H. C., 1976, Application of the U.S. Geological Survey rainfall-runoff simulation model to improve flood-frequency estimates on small Tennessee streams: U.S. Geological Survey Water-Resources Investigations 76-120, 53 p.

Table 1.--Model parameters and variables and their application in the modeling process

Parameter	Variable	Units	Application
<i>BMSM</i> -----	-----	Inches----	Soil-moisture storage at field capacity. Maximum value of base moisture storage variable, <i>BMS</i> .
<i>RR</i> -----	-----	0.85*-----	Proportion of daily rainfall that infiltrates the soil.
<i>EVC</i> -----	-----	0.65-0.75*	Pan evaporation coefficient.
<i>DRN</i> -----	-----	1.0*-----	Drainage factor for redistribution of saturated moisture storage, <i>SMS</i> , to base (unsaturated) moisture storage, <i>BMS</i> , as a fraction of hydraulic conductivity, <i>KSAT</i> .
-----	<i>BMS</i> -----	Inches----	Base (unsaturated) moisture storage in active soil column. Simulates antecedent moisture content over the range from wilting-point conditions, <i>BMS</i> =0, to field capacity, <i>BMS</i> = <i>BMSM</i> .
-----	<i>SMS</i> -----	Inches----	"Saturated" moisture storage in wetted surface layer developed by infiltration of storm rainfall.
-----	<i>FR</i> -----	Inches per hour----	Infiltration capacity, a function of <i>KSAT</i> , <i>PSP</i> , <i>RGF</i> , <i>BMSM</i> , <i>SMS</i> , <i>BMS</i> (equation 4).
<i>KSAT</i> -----	-----	Inches per hour----	Hydraulic conductivity of "saturated" transmission zone.
<i>PSP</i> -----	-----	Inches----	Combined effects of moisture deficit, as indexed by <i>BMS</i> , and capillary potential (suction) at the wetting front for <i>BMS</i> equal to field capacity, <i>BMSM</i> .
<i>RGF</i> -----	-----	-----	Ratio of combined effects of moisture deficit, as indexed by <i>BMS</i> , and capillary potential (suction) at wetting front for <i>BMS</i> =0=wilting point, to the value associated with field capacity conditions, <i>PSP</i> .
<i>KSW</i> -----	-----	Hours----	Linear reservoir recession coefficient.
<i>TC</i> -----	-----	Minutes---	Time base (duration) of triangular translation hydrograph.
<i>TP/TC</i> ----	-----	0.5*-----	Ratio of time to peak of triangular translation hydrograph to duration of translation hydrograph, <i>TC</i> .
-----	<i>SW</i> -----	Inches----	Linear reservoir storage.

*The parameters *RR* and *EVC* are highly "interactive" and were constrained. *RR* was arbitrarily assigned the value of 0.85, and *EVC* values were computed as the factor required to scale available local average annual pan evaporation to equivalent values of average annual lake evaporation as estimated from figure 2, "Evaporation maps for the United States," Technical Paper No. 37, U.S. Department of Commerce, 1959. The parameters *DRN* and *TP/TC* have little influence on model results. *DRN* was arbitrarily assigned a value of 1.0, and the shape of an isosceles triangle assumed for the translation hydrograph.

Table 2.--Long-term recording rainfall sites used in study
 [NS, number of storm events; NYW, number of water years]

Rain-gage location	Period of record	NS	NYW*
Dubuque, Iowa-----	1903-71-----	129	69
Chicago, Ill.-----	1902-74-----	168	73
Peoria, Ill.-----	1905-74-----	352	70
Springfield Ill.---	1904-51, 1953-74-----	177	70
Atlantic City, N.J.	1900-14, 1919-58-----	165	55
Baltimore, Md.-----	1900-71-----	221	72
Kansas City, Mo.---	1893-1933, 1935-70-----	231	67
Columbia, Mo.-----	1898-1970-----	221	73
St. Louis, Mo.-----	1893-97, 1899, 1902, 1905, 1907-65, 1969-----	187	66
Louisville, Ky.---	1912-62-----	274	51
Richmond, Va.-----	1898-1969-----	156	72
Lynchburg, Va.-----	1902-21, 1923-33, 1937-39-----	162	64
Springfield, Mo.---	1905-13, 1915-70-----	180	60
Cairo, Ill.-----	1908-74-----	166	67
Wytheville, Va.-----	1905-14, 1916-42, 1944-47, 1951-52, 1954-63, 1965-70	129	59
Nashville, Tenn.---	1898-1970-----	250	73
Knoxville, Tenn.---	1898-1970-----	313	73
Charlotte, N.C.---	1902-69-----	684	68
Memphis, Tenn.-----	1898, 1900-18, 1920-30, 1932-71-----	359	71
Chattanooga, Tenn.-	1901-73-----	339	73
Greenville, S.C.---	1918-33, 1939-71-----	139	49
Little Rock, Ark.--	1898-1970-----	370	73
Columbia, S.C.-----	1901-54-----	143	54
Atlanta, Ga.-----	1898-1973-----	332	76
Birmingham, Ala.---	1904-73-----	350	70
Augusta, Ga.-----	1902-73-----	377	72
Macon, Ga.-----	1900-73-----	443	74
Shreveport, La.---	1913-52, 1960-72-----	277	53
Vicksburg, Miss.---	1898-1948, 1950-55, 1957-67-----	146	68
Montgomery, Ala.---	1897-1313, 1915-50-----	167	53
Meridian, Miss.---	1900-67-----	331	68
Savannah, Ga.-----	1898-1973-----	429	76
Thomasville, Ga.---	1906-33, 1941-73-----	265	61
Jacksonville, Fla.-	1905-72-----	345	68
Pensacola, Fla.---	1903-68-----	278	66
New Orleans, La.---	1912-72-----	340	61

*Annual flood synthesis requires daily precipitation values during nonstorm moisture accounting periods and 5-minute rainfall intensities during storm events (fig. 1). A "storm event" is a subjective definition and may comprise several hours of intense rainfall occurring within a period of several consecutive days. Dates of storm events were identified by U.S. Geological Survey personnel by analysis of available precipitation summaries. The majority of the storm event data were coded from original recorder charts by the National Climatic Data Center, NOAA, Asheville, N.C. In some instances copies of original recorder charts were acquired and reduction made by U.S. Geological Survey personnel. Streamflow characteristics such as the annual peak discharge, mean annual flow, and so forth, are typically reported on a water-year basis. The water year, October 1 through September 30, is identified by the calendar year in which it ends.

Table 3.--Streamflow stations used in study

Map code ¹ , station no., name, location, and number of observed annual floods	Rainfall-runoff model parameters						Parameters used in map-model estimating procedure ²					
	PSP (in)	KSAT (in/h)	RGF (in)	BMSM (in)	KSW (h)	TC (h)	Area (mi ²)	L (h)	F (in/h)	C ₂	C ₂₅	C ₁₀₀
D01 02191280 Mill Shoal Creek near Royston, Ga.	12	0.66	0.105	25.8	4.59	0.57	0.73	0.32	0.94	0.27	175	660
D02 02191930 Buffalo Creek near Lexington, Ga.	12	.65	.089	14.2	6.08	3.53	4.94	5.80	6.00	.18	185	950
D03 02215245 Folsom Creek Tributary near Rochelle, Ga.	12	1.03	.098	32.1	7.58	3.12	4.65	1.44	5.45	.39	250	860
D04 02225210 Hurricane Branch near Wrightville, Ga.	10	1.91	.054	14.9	3.10	7.27	7.40	3.53	11.0	.21	225	800
D05 02327350 Ochlocknee River Tributary near Coolidge, Ga.	11	.71	.029	26.4	4.04	5.22	4.02	1.81	7.23	.079	300	940
D06 02343700 Stevenson Creek near Headland, Ala.	15	5.42	.145	4.1	9.09	3.10	4.50	12.4	5.35	.72	310	980
D07 02346217 Celeoth Creek near Manchester, Ga.	7	3.29	.191	9.7	3.32	2.27	1.97	2.82	3.25	.92	225	820
D08 02381600 Faucett Creek near Talking Rock, Ga.	10	6.76	.061	13.8	9.66	5.40	3.00	9.99	6.90	.66	185	640
D09 02384600 Mill Creek Tributary near Eton, Ga.	11	.87	.097	4.9	2.30	4.25	5.50	4.28	7.00	.16	185	900
D10 02388200 Storey Mill Creek near Summerville, Ga.	10	1.45	.074	5.0	9.06	4.86	3.74	6.02	6.73	.16	210	660
D11 02399800 Little Terrapin Creek near Borden Springs, Ala.	8	1.95	.070	15.5	3.90	8.13	6.50	15.9	11.4	.29	230	740
D12 02410000 Patterson Creek near Central, Ala.	24	7.85	.081	16.2	6.60	1.50	1.75	4.95	2.38	1.12	285	900
D13 02413400 Wedowee Creek above Wedowee, Ala.	13	3.35	.091	10.3	2.51	1.80	4.00	6.50	3.80	.46	250	800
D14 02427300 Prairie Creek near Oak Hill, Ala.	14	2.19	.037	15.7	2.02	5.00	4.00	9.73	7.00	.17	325	980
D15 02435400 Clear Branch near Tupelo, Miss.	20	2.70	.049	15.6	3.07	2.44	3.73	.75	4.31	.26	260	725
D16 02437800 Barn Creek near Hackelburg, Ala.	14	1.26	.067	21.0	5.65	8.00	5.00	12.9	10.5	.24	265	740
D17 02441220 Sand Creek Tributary near Mayhew, Miss.	10	1.01	.034	10.1	2.70	1.50	1.25	.44	2.12	.075	280	810
D18 02449400 Jones Creek near Epes, Ala.	16	1.27	.032	11.9	2.21	1.85	5.00	11.7	4.35	.087	310	925
D19 02451750 Vest Creek near Baldwin, Ala.	9	2.92	.087	14.6	6.48	1.25	1.25	1.64	1.88	.47	260	725
D20 02462600 Blue Creek near Oakman, Ala.	14	2.40	.069	40.1	6.60	6.00	2.00	5.70	4.00	.64	280	810
D21 02479165 Mosquito Branch at Bemudala, Miss.	21	2.84	.036	7.9	1.14	1.95	4.05	.22	3.98	.14	450	1,400
D22 02482900 Tallahogue Creek Tributary near Harpersville, Miss.	10	3.34	.059	10.0	5.23	.99	.55	.12	1.27	.29	300	950
D23 03344250 Embarras River Tributary near Greenup, Ill.	20	.78	.027	24.6	1.31	1.66	.40	.081	1.86	.075	145	545
D24 03435600 Sulphur Fork River Tributary near Whitehouse, Tenn.	8	5.75	.097	17.6	4.97	.65	.83	3.50	1.07	1.07	180	575
D25 03461200 Cosby Creek above Cosby, Tenn.	17	4.08	.073	22.2	1.04	2.30	3.17	10.2	3.88	.69	135	560
D26 03486225 Powder Branch near Johnson City, Tenn.	4	6.36	.156	22.9	6.24	.55	1.17	4.88	1.14	1.48	110	460
D27 03535180 Willow Fork near Halls Crossroads, Tenn.	9	5.72	.085	7.1	7.32	1.75	2.67	3.23	3.08	.55	135	525
D28 03539100 Byrd Creek near Crossville, Tenn.	9	4.05	.135	10.1	3.26	1.57	3.10	1.10	3.12	.78	170	575
D29 03597500 Wartrace Creek at Bell Buckle, Tenn.	22	2.02	.030	9.0	2.92	1.25	4.17	16.3	3.33	.098	200	600

Table 3.--Streamflow stations used in study--Continued

Map code ¹ , station no., name, location, and number of observed annual floods	Rainfall-runoff model parameters						Parameters used in map-model estimating procedure ²					
	PSP (in)	KSAT (in/h)	BMSM (in)	KSW (h)	TC (h)	Area (mi ²)	L (h)	F (in/h)	C ₂	C ₂₅	C ₁₀₀	
D30 03604070	9	6.48	0.150	24.6	3.14	1.10	1.33	1.77	2.36	210	620	875
Tenn.-----												
D31 05439550	17	2.81	.095	12.7	1.46	.80	1.83	1.71	.46	125	560	800
South Branch Kishwaukee River Tributary near Irene, Ill.-----												
D32 05448050	20	3.31	.172	15.5	8.16	.42	1.12	.22	1.08	135	600	875
Sand Creek near Milan, Ill.-----												
D33 05502120	20	1.92	.051	11.8	1.18	.57	.98	.78	.18	155	510	725
Kiser Creek Tributary near Barry, Ill.-----												
D34 05503000	19	1.41	.033	19.7	2.00	1.75	1.25	2.64	.12	140	540	750
Oak Dale Branch near Emden, Mo.-----												
D35 05527050	17	1.08	.050	5.7	1.69	1.50	4.17	.83	.097	120	500	650
Prairie Creek near Frankfort, Ill.-----												
D36 05566000	23	1.28	.050	39.2	4.99	7.50	3.42	6.30	.27	130	510	700
East Branch Panther Creek near Gridley, Ill.-----												
D37 05587850	20	3.49	.055	18.2	3.00	.71	.55	.45	.40	165	650	1,000
Cahokia Creek Tributary near Carpenter, Ill.-----												
D38 05599640	19	4.49	.135	23.0	1.32	.32	.27	.44	1.44	175	725	1,150
Green Creek Tributary near Jonesboro, Ill.-----												
D39 06816000	25	3.54	.082	10.3	5.75	.65	1.10	4.90	.43	125	750	1,200
Mill Creek near Oregon, Mo.-----												
D40 06902800	20	5.20	.045	22.4	6.64	1.75	1.33	1.04	.54	135	660	1,000
Onion Branch near St. Catherine, Mo.-----												
D41 06910250	17	1.83	.043	11.6	5.93	.50	.50	.55	.14	140	500	700
Traxler Branch near Columbia, Mo.-----												
D42 06921740	14	1.96	.041	6.1	5.92	.75	.50	1.15	.11	130	650	975
Brushy Creek near Blairstown, Mo.-----												
D43 07015500	20	.64	.032	6.3	4.39	.94	1.50	.22	.051	150	630	925
Lanes Fork near Rolla, Mo.-----												
D44 07028940	9	1.40	.031	15.3	4.02	.98	2.25	7.87	.099	210	640	900
Turkey Creek near Medina, Tenn.-----												
D45 07030365	10	3.60	.056	11.6	3.13	2.88	4.13	2.17	.32	235	650	925
Wesley Branch near Walnut, Miss.-----												
D46 07054200	19	4.90	.144	15.0	4.35	.66	.50	.33	1.24	125	640	925
Yandell Branch near Kirbyville, Mo.-----												
D47 07063200	15	1.95	.061	6.7	6.00	.63	.33	.28	.17	185	750	1,050
Pike Creek Tributary near Poplar Bluff, Mo.-----												
D48 07277550	10	1.13	.012	2.4	1.22	.82	.67	.29	.020	240	675	950
James Wolf Creek Tributary near Looxahoma, Miss.-----												
D49 07287140	7	1.05	.013	2.6	6.44	2.70	1.80	.26	.022	265	750	1,100
Martin Lake Tributary at Sidon, Miss.-----												
D50 07373550	20	1.36	.023	7.6	3.59	.79	.74	.21	.054	325	1,100	1,600
Moore's Branch near Woodville, Miss.-----												
T01 02192300	17	1.37	.047	12.1	3.05	.70	.92	.097	.14	180	650	925
Hog Fork Fishing Creek Tributary near Tignall, Ga.-----												
T02 02202910	11	1.51	.137	18.7	4.60	4.18	3.15	1.14	.52	270	850	1,250
Ten Mile Creek Tributary at Pulaski, Ga.-----												
T03 02216610	10	1.21	.103	10.8	6.46	4.44	5.85	3.23	.26	265	860	1,250
Ocmulgee River Tributary near Lumber City, Ga.-----												
T04 02217400	11	2.23	.109	3.2	8.53	1.89	2.00	2.68	.27	185	670	950
Mulberry River Tributary near Winder, Ga.-----												
T05 02226150	11	.58	.065	20.4	7.93	18.58	10.56	6.38	.14	285	900	1,275
Satilla River Tributary near Willacoochee, Ga.-----												

Table 3.--Streamflow stations used in study--Continued

Map code ¹ , station no., name, location, and number of observed annual floods	Rainfall-runoff model parameters						Parameters used in map-model estimating procedure ²						
	FSP (in)	KSAT (in/h)	RGF (in)	BMSM (in)	KSW (h)	TC (h)	Area (mi ²)	L (h)	F (in/h)	C ₂	C ₂₅	C ₁₀₀	
T06 02317710 Withlacoochee River Tributary near Nashville, Ga.	16	1.50	0.116	12.2	7.95	5.30	3.30	0.86	6.95	0.35	300	925	1,300
T07 02317845 Warrior Creek Tributary near Sylvester, Ga.	10	1.72	.038	22.3	8.43	5.60	3.20	1.64	7.20	.18	270	900	1,275
T08 02342200 Phelps Creek near Opelika, Ala.	16	2.28	.103	13.3	4.06	4.75	2.50	7.47	6.00	.44	270	860	1,225
T09 02371200 Indian Creek near Troy, Ala.	17	5.72	.154	5.5	6.60	6.50	7.00	8.88	10.0	.90	310	975	1,400
T10 02387200 Beamer Creek near Spring Place, Ga.	11	.37	.018	3.5	3.26	2.07	2.23	1.29	3.19	.024	170	640	925
T11 02387560 Oothkaaloga Creek Tributary at Adairsville, Ga.	10	2.70	.103	17.8	7.16	2.38	2.00	3.56	3.38	.59	200	675	950
T12 02407900 Paint Creek near Marble Valley, Ala.	12	5.26	.086	8.6	6.50	4.50	4.23	13.5	6.67	.57	285	850	1,200
T13 02414800 Harbuck Creek near Hackneyville, Ala.	20	5.04	.057	4.3	2.83	2.50	2.75	6.70	3.88	.28	270	825	1,150
T14 02421300 Ivy Creek near Mulberry, Ala.	12	9.11	.092	8.2	5.44	4.50	5.00	10.5	7.00	.97	300	925	1,300
T15 02428300 Tallatchee Creek near Vredenburgh, Ala.	16	1.54	.059	24.1	6.60	4.50	7.00	14.6	8.00	.26	335	1,050	1,500
T16 02437900 Woods Creek near Hamilton, Ala.	12	2.75	.102	9.3	4.80	7.00	3.50	14.1	8.75	.42	260	740	1,000
T17 02450200 Dorsey Creek near Arkadelphia, Ala.	16	1.89	.046	10.7	6.32	8.50	3.50	13.0	10.3	.15	260	750	1,050
T18 02465205 Jay Creek near Coker, Ala.	10	4.97	.108	13.9	5.24	2.50	1.50	3.56	3.25	.90	285	850	1,200
T19 02469672 Little Okatuppa Creek near Quitman, Miss.	10	2.16	.031	9.2	5.51	2.77	3.53	4.35	4.54	.11	335	1,000	1,450
T20 02472810 Okatoma Creek Tributary No. 2 near Collins, Miss.	9	1.02	.045	18.0	3.60	1.00	1.00	.206	1.50	.13	340	1,100	1,550
T21 02483890 Yockanookany River Tributary near McCool, Miss.	11	1.68	.022	6.1	5.52	1.70	1.39	.34	2.40	.055	235	840	1,200
T22 02489030 Elmers Draw near Columbia, Miss.	21	3.24	.033	16.7	1.82	1.80	.65	.91	2.13	.21	350	1,225	1,650
T23 03313600 West Fork Drakes Creek Tributary near Fountain Head, Tenn.	9	3.30	.088	15.3	5.50	.67	.83	.95	1.09	.55	175	550	775
T24 03338100 Salt Creek Tributary near Catlin, Ill.	17	1.71	.054	24.9	1.92	2.54	2.90	2.20	3.99	.27	125	505	700
T25 03380300 Dums Creek Tributary near Iuka, Ill.	20	3.33	.040	16.3	1.50	.086	.75	.078	.46	.26	160	625	825
T26 03381600 Little Wabash River Tributary near New Haven, Ill.	16	3.49	.075	16.1	1.17	.214	.77	.156	.60	.51	170	625	800
T27 03420360 Mud Creek Tributary No. 2 near Summitville, Tenn.	9	2.30	.076	9.2	3.04	2.75	3.67	2.28	4.58	.27	190	600	875
T28 03430400 Mill Creek at Nolensville, Tenn.	11	1.26	.020	13.3	3.07	.64	2.08	12.0	1.68	.056	190	575	825
T29 03519650 Little Baker Creek near Greenback, Tenn.	9	5.98	.139	13.9	2.03	1.50	1.50	3.65	2.25	1.36	175	575	925
T30 03541100 Bitter Creek near Camp Austin, Tenn.	9	2.98	.095	7.7	2.58	1.17	1.45	5.53	1.90	.38	175	550	850
T31 05469750 Ellison Creek Tributary near Roseville, Ill.	20	2.65	.131	16.9	6.00	.63	1.23	.26	1.25	.72	140	575	800

Table 3.--Streamflow stations used in study--Continued

Map code ¹ , station no., name, location, and number of observed annual floods	Rainfall-runoff model parameters						Parameters used in map-model estimating procedure ²					
	PSP (in)	KSAT (in/h)	RGF (in)	BMSM (in)	KSW (h)	TC (h)	Area (mi ²)	L (h)	F (in/h)	C ₂	C ₂₅	C ₁₀₀
T32 05495200 Little Creek near Breckenridge, Ill.-----	20 1.41	0.070	21.9	3.07	0.72	1.13	1.45	1.29	0.27	145	550	750
T33 05558075 Coffee Creek Tributary near Hennepin, Ill.-----	20 3.88	.081	11.7	5.99	.106	1.06	.22	.63	.49	135	520	725
T34 05577700 Sangamon River Tributary at Andrew, Ill.-----	20 2.70	.095	27.9	2.26	1.44	1.10	1.50	1.99	.75	150	540	775
T35 05595550 Marys River Tributary at Chester, Ill.-----	15 4.17	.070	10.0	1.53	.51	.49	.65	.76	.42	170	725	1,150
T36 06821000 Jenkins Branch near Gower, Mo.---	25 1.31	.060	13.8	4.64	.75	.75	2.72	1.13	.18	125	750	1,150
T37 06896500 Thompson Branch near Albany, Mo.---	17 1.02	.044	5.8	1.95	2.00	2.25	5.58	3.12	.084	125	750	1,200
T38 06908300 Trent Branch near Waverly, Mo.---	20 1.97	.059	14.9	4.35	.34	.75	.97	.71	.24	135	650	1,000
T39 06925300 Prairie Branch near Decaturville, Mo.-----	20 4.03	.126	14.2	6.00	1.25	.58	1.48	1.54	.88	130	550	850
T40 07028930 Turkey Creek at Medina, Tenn.-----	9 2.20	.048	16.3	4.88	.75	1.92	4.75	1.71	.22	210	630	900
T41 07035500 Barnes Creek near Fredericktown, Mo.-----	19 2.16	.043	14.5	4.28	.75	1.25	4.03	1.38	.18	170	725	1,150
T42 07064500 Big Creek near Yukon, Mo.-----	25 2.36	.036	8.2	2.02	1.70	1.25	8.36	2.32	.12	160	690	1,000
T43 07068200 North Prong Little Black River near Hunter, Mo.-----	17 12.40	.132	16.8	6.70	1.09	1.00	1.23	1.59	2.89	180	750	1,075
T44 07185500 Stahl Creek near Miller, Mo.-----	24 1.71	.048	24.8	3.52	1.50	1.75	3.86	2.38	.24	115	590	875
T45 07267200 Cracker Ditch near Pontotoc, Miss.---	19 1.40	.018	5.9	4.86	1.89	1.39	.23	2.58	.040	255	710	975
T46 07283490 Caney Creek near Coffeerville, Miss.-----	21 3.24	.035	19.3	7.94	.61	2.70	1.97	1.96	.25	260	750	1,025
T47 07287520 Short Creek Tributary near Yazoo City, Miss.-----	9 1.36	.023	16.7	2.02	1.05	1.20	1.49	1.65	.076	285	860	1,250
T48 07290525 White Oak Creek Tributary near Utica, Miss.-----	11 1.40	.028	15.1	3.76	1.33	2.85	1.36	2.76	.089	300	960	1,450
T49 07294400 Observers Draw near Doloroso, Miss.-----	20 3.28	.048	11.2	3.64	.88	.28	.22	1.02	.25	315	1,025	1,550

¹Map codes D01 through D50 identify those stations used to develop synthetic annual floods. Codes T01 through T49 identify the other stations included in the evaluation of the map-model estimating procedure.

²See text for a discussion of the hydrograph shape factor, *L*, the infiltration factor, *F*, and the climatic factors, *C*₂, *C*₂₅, and *C*₁₀₀.

³This station was not included in the evaluation of the map-model estimating procedure because the record length is too short.

Table 4.--Results of multiple-regression analysis for rural model applications

Rain-gage location	2-yr recurrence interval				25-yr recurrence interval				100-yr recurrence interval						
	a	b ₁	b ₂	Standard error	a	b ₁	b ₂	Standard error	a	b ₁	b ₂	Standard error			
				log ₁₀ Percent				log ₁₀ Percent				log ₁₀ Percent			
Dubuque, Iowa	137	-0.72	-0.56	0.094	21.9	738	-0.73	-0.23	0.057	13.1	1230	-0.75	-0.14	0.047	10.8
Chicago, Ill.	124	-0.73	-0.56	0.090	21.0	504	-0.70	-0.28	0.053	12.1	678	-0.67	-0.21	0.043	9.9
Peoria, Ill.	155	-0.75	-0.51	0.081	18.7	543	-0.70	-0.22	0.040	9.2	776	-0.68	-0.12	0.035	8.0
Springfield, Ill.	132	-0.73	-0.54	0.086	20.0	574	-0.75	-0.25	0.043	9.9	857	-0.75	-0.17	0.037	8.4
Atlantic City, N.J.	113	-0.63	-0.55	0.077	17.7	783	-0.63	-0.21	0.050	11.5	1600	-0.64	-0.10	0.049	11.4
Baltimore, Md.	135	-0.70	-0.55	0.091	21.1	565	-0.69	-0.30	0.066	15.3	783	-0.66	-0.24	0.063	14.5
Kansas City, Mo.	128	-0.73	-0.58	0.105	24.4	692	-0.69	-0.24	0.053	12.3	1110	-0.66	-0.14	0.041	9.3
Columbia, Mo.	149	-0.74	-0.53	0.087	20.3	527	-0.74	-0.26	0.048	11.0	740	-0.75	-0.18	0.049	11.3
St. Louis, Mo.	144	-0.74	-0.52	0.083	19.2	698	-0.69	-0.21	0.037	8.6	1110	-0.65	-0.12	0.031	7.1
Louisville, Ky.	132	-0.69	-0.49	0.074	17.2	469	-0.72	-0.25	0.029	6.7	679	-0.71	-0.17	0.034	7.8
Richmond, Va.	126	-0.72	-0.58	0.097	22.6	615	-0.71	-0.30	0.065	15.0	957	-0.67	-0.22	0.054	12.5
Lynchburg, Va.	71.0	-0.67	-0.67	0.102	23.7	437	-0.75	-0.36	0.071	16.3	759	-0.76	-0.26	0.062	14.3
Springfield, Mo.	112	-0.71	-0.58	0.095	22.0	565	-0.68	-0.24	0.048	11.1	889	-0.66	-0.14	0.042	9.6
Cairo, Ill.	199	-0.64	-0.40	0.061	14.0	734	-0.65	-0.19	0.038	8.6	1090	-0.66	-0.14	0.039	8.9
Wytheville, Va.	55.7	-0.62	-0.70	0.100	23.1	413	-0.81	-0.33	0.065	14.9	760	-0.88	-0.21	0.057	13.1
Nashville, Tenn.	183	-0.65	-0.41	0.060	13.8	615	-0.73	-0.21	0.034	7.9	837	-0.77	-0.18	0.038	8.8
Knoxville, Tenn.	139	-0.64	-0.45	0.067	15.4	598	-0.74	-0.23	0.040	9.1	966	-0.76	-0.17	0.041	9.5
Charlotte, N.C.	162	-0.79	-0.49	0.080	18.5	531	-0.76	-0.24	0.041	9.5	729	-0.73	-0.17	0.032	7.3
Memphis, Tenn.	217	-0.65	-0.37	0.033	12.2	652	-0.66	-0.19	0.033	7.6	904	-0.66	-0.16	0.037	8.5
Chattanooga, Tenn.	225	-0.70	-0.34	0.049	11.4	685	-0.75	-0.18	0.025	5.6	940	-0.77	-0.16	0.028	6.5
Greenville, S.C.	182	-0.65	-0.42	0.063	14.6	685	-0.70	-0.25	0.043	10.0	973	-0.71	-0.22	0.051	11.7
Little Rock, Ark.	242	-0.67	-0.37	0.063	14.5	738	-0.65	-0.17	0.032	7.3	953	-0.65	-0.14	0.042	9.7
Columbia, S.C.	120	-0.70	-0.58	0.101	23.5	542	-0.73	-0.29	0.052	12.0	755	-0.72	-0.21	0.043	9.9
Atlanta, Ga.	230	-0.72	-0.38	0.061	14.1	753	-0.76	-0.20	0.035	8.1	1010	-0.76	-0.18	0.045	10.3
Birmingham, Ala.	307	-0.69	-0.30	0.045	10.4	830	-0.67	-0.16	0.037	8.5	1090	-0.66	-0.14	0.045	10.3
Augusta, Ga.	184	-0.74	-0.48	0.078	18.1	665	-0.74	-0.24	0.040	9.3	935	-0.74	-0.18	0.039	8.9
Macon, Ga.	224	-0.75	-0.40	0.062	14.3	815	-0.72	-0.20	0.032	7.5	1190	-0.71	-0.16	0.038	8.7
Shreveport, La.	245	-0.71	-0.41	0.074	17.0	685	-0.63	-0.18	0.030	7.0	859	-0.60	-0.12	0.036	8.3
Vicksburg, Miss.	288	-0.64	-0.30	0.050	11.4	900	-0.59	-0.16	0.032	7.3	1190	-0.56	-0.14	0.035	8.0
Montgomery, Ala.	313	-0.70	-0.32	0.054	12.4	998	-0.65	-0.14	0.031	7.1	1250	-0.61	-0.12	0.037	8.5
Meridian, Miss.	366	-0.70	-0.29	0.050	11.4	885	-0.72	-0.19	0.033	7.5	1100	-0.72	-0.19	0.043	9.8
Savannah, Ga.	341	-0.75	-0.35	0.062	14.3	1240	-0.68	-0.11	0.034	7.7	1710	-0.66	-0.06	0.038	8.6
Thomasville, Ga.	332	-0.74	-0.35	0.062	14.4	952	-0.68	-0.15	0.025	5.6	1230	-0.65	-0.10	0.030	6.8
Jacksonville, Fla.	400	-0.77	-0.31	0.055	12.6	1140	-0.68	-0.11	0.030	6.9	1430	-0.63	-0.07	0.040	9.2
Pensacola, Fla.	475	-0.69	-0.27	0.046	10.5	1500	-0.64	-0.11	0.031	7.2	2130	-0.61	-0.08	0.036	8.3
New Orleans, La.	482	-0.70	-0.28	0.051	11.7	1340	-0.59	-0.10	0.030	6.9	1800	-0.54	-0.06	0.032	7.3

Table 5.--Summary and comparison of multiple-regression (m-r) and direct-search (d-s) determinations for the coefficient, a_i

Rain-gage location	2-yr recurrence interval					25-yr recurrence interval					100-yr recurrence interval							
	Standard error		Percent		a	Standard error		Percent		a	Standard error		Percent		a			
	m-r	d-s	log ₁₀	m-r		d-s	m-r	d-s	log ₁₀		m-r	d-s	m-r	d-s		log ₁₀	m-r	d-s
Dubuque, Iowa	137	140	0.094	0.096	21.9	22.2	738	720	0.057	0.058	13.1	13.2	1230	1170	0.047	0.050	10.8	11.4
Chicago, Ill.	124	121	0.090	0.092	21.0	21.0	504	504	0.052	0.052	12.1	11.9	678	678	0.043	0.044	9.9	10.1
Peoria, Ill.	155	151	0.081	0.081	18.7	18.8	543	504	0.040	0.050	9.2	11.5	776	720	0.035	0.059	8.0	13.5
Springfield, Ill.	132	129	0.086	0.086	20.0	19.8	574	533	0.043	0.049	9.9	11.2	857	775	0.037	0.046	8.4	10.5
Atlantic City, N.J.	113	122	0.077	0.080	17.7	18.3	783	844	0.050	0.056	11.5	12.7	1600	1770	0.049	0.057	11.4	13.0
Baltimore, Md.	135	138	0.091	0.091	21.1	21.1	565	579	0.066	0.069	15.3	16.0	783	865	0.063	0.069	14.5	15.7
Kansas City, Mo.	128	131	0.105	0.108	24.4	25.0	692	710	0.053	0.054	12.3	12.4	1110	1140	0.040	0.046	9.3	10.6
Columbia, Mo.	149	149	0.087	0.089	20.3	20.3	527	489	0.048	0.053	11.0	12.1	740	670	0.049	0.060	11.3	13.8
St. Louis, Mo.	144	140	0.083	0.083	19.2	19.1	698	698	0.037	0.038	8.6	8.6	1110	1170	0.031	0.036	7.1	8.2
Louisville, Ky.	132	129	0.074	0.076	17.2	17.5	469	424	0.029	0.045	6.7	10.4	679	614	0.034	0.053	7.8	12.2
Richmond, Va.	126	129	0.097	0.100	22.6	23.2	615	631	0.065	0.071	15.0	16.7	957	1060	0.054	0.065	12.5	14.9
Lynchburg, Va.	71.0	77.2	0.102	0.105	23.7	24.1	437	448	0.071	0.076	16.3	17.6	759	759	0.062	0.070	14.3	15.9
Springfield, Mo.	112	115	0.095	0.095	22.0	22.0	565	565	0.048	0.049	11.1	11.2	889	889	0.042	0.049	9.6	11.1
Cairo, Ill.	199	199	0.061	0.067	14.0	15.4	734	753	0.037	0.042	8.6	9.5	1090	1150	0.039	0.041	8.9	9.5
Wytheville, Va.	55.7	63.1	0.099	0.106	23.1	24.4	413	364	0.065	0.077	14.9	17.6	760	607	0.057	0.092	13.1	21.2
Nashville, Tenn.	183	178	0.060	0.068	13.8	15.5	615	571	0.034	0.044	7.9	10.2	837	757	0.038	0.050	8.8	11.5
Knoxville, Tenn.	139	139	0.067	0.076	15.4	17.4	598	555	0.039	0.045	9.1	10.3	966	896	0.041	0.048	9.5	11.0
Charlotte, N.C.	162	147	0.080	0.085	18.5	19.6	631	480	0.041	0.054	9.5	12.2	729	660	0.032	0.046	7.3	10.6
Memphis, Tenn.	217	212	0.053	0.065	12.2	14.9	652	652	0.033	0.041	7.6	9.5	904	904	0.037	0.039	8.5	9.0
Chattanooga, Tenn.	225	204	0.049	0.073	11.4	16.6	685	604	0.024	0.047	5.6	10.8	940	851	0.028	0.043	6.5	9.8
Greenville, S.C.	182	182	0.063	0.068	14.6	15.5	685	702	0.043	0.044	10.0	10.3	973	998	0.051	0.059	11.7	14.0
Little Rock, Ark.	242	236	0.063	0.066	14.5	15.1	738	738	0.032	0.040	7.3	9.1	953	953	0.042	0.046	9.7	10.6
Columbia, S.C.	120	123	0.103	0.102	24.0	23.7	542	529	0.052	0.053	12.0	12.2	755	736	0.043	0.043	9.9	9.9
Atlanta, Ga.	230	213	0.061	0.068	14.1	15.6	753	699	0.035	0.042	8.1	9.6	1010	961	0.044	0.049	10.3	11.3
Birmingham, Ala.	307	285	0.045	0.061	10.4	13.9	830	809	0.037	0.042	8.5	9.6	1090	1120	0.044	0.046	10.3	10.5
Augusta, Ga.	184	179	0.078	0.079	18.1	18.1	665	649	0.040	0.043	9.3	9.8	935	912	0.039	0.041	8.9	9.4
Macon, Ga.	224	203	0.062	0.069	14.3	15.7	815	795	0.032	0.034	7.5	7.7	1190	1220	0.038	0.040	8.7	9.3
Shreveport, La.	245	239	0.073	0.073	17.0	16.7	685	685	0.030	0.044	7.0	10.1	859	903	0.036	0.057	8.3	13.0
Vicksburg, Miss.	288	281	0.049	0.066	11.4	15.1	900	995	0.032	0.049	7.3	11.3	1190	1420	0.035	0.067	8.0	15.4
Montgomery, Ala.	313	298	0.054	0.061	12.4	13.9	998	1020	0.031	0.037	7.1	8.4	1250	1380	0.037	0.050	8.5	11.4
Meridian, Miss.	366	348	0.049	0.057	11.4	13.1	885	885	0.033	0.033	7.5	7.5	1100	1130	0.043	0.047	9.8	11.1
Savannah, Ga.	341	324	0.062	0.065	14.3	14.9	1240	1240	0.034	0.034	7.7	7.7	1710	1800	0.037	0.040	8.6	9.1
Thomasville, Ga.	332	316	0.062	0.064	14.4	14.7	652	952	0.024	0.024	5.6	6.3	1230	1260	0.030	0.036	6.8	7.9
Jacksonville, Fla.	400	362	0.055	0.063	12.6	14.3	1140	1110	0.030	0.034	6.9	7.7	1430	1500	0.040	0.047	9.2	10.8
Pensacola, Fla.	475	463	0.046	0.048	10.5	10.9	1500	1660	0.031	0.043	7.2	9.8	2130	2470	0.036	0.064	8.3	14.7
New Orleans, La.	482	470	0.051	0.051	11.7	11.7	1340	1520	0.030	0.050	6.9	11.5	1800	2140	0.032	0.071	7.3	16.2

Table 6.---Results of the direct-search determinations for the coefficient, d_i , for effect of impervious area

Rain-gage location	2-yr recurrence interval			25-yr recurrence interval			100-yr recurrence interval		
	a	d	log ₁₀ Percent	a	d	log ₁₀ Percent	a	d	log ₁₀ Percent
Dubuque, Iowa	140	5.61	0.052	720	1.91	0.047	1,170	1.43	0.050
Chicago, Ill.	121	5.70	0.056	504	2.26	0.041	678	2.09	0.047
Peoria, Ill.	151	4.78	0.050	504	2.15	0.038	720	1.65	0.041
Springfield, Ill.	129	5.12	0.052	533	2.19	0.038	775	1.94	0.034
Atlantic City, N.J.	122	5.61	0.050	844	1.73	0.048	1,770	1.11	0.057
Baltimore, Md.	138	5.29	0.052	579	2.60	0.046	865	2.25	0.049
Kansas City, Mo.	131	5.72	0.058	710	2.12	0.042	1,140	1.76	0.043
Columbia, Mo.	149	4.89	0.053	489	2.39	0.037	670	2.08	0.038
St. Louis, Mo.	140	4.98	0.050	698	1.91	0.033	1,170	1.57	0.035
Louisville, Ky.	129	4.63	0.050	424	2.29	0.032	614	1.76	0.032
Richmond, Va.	129	5.81	0.054	631	2.42	0.052	1,060	1.82	0.058
Lynchburg, Va.	77.2	7.80	0.055	448	2.68	0.052	759	2.00	0.055
Springfield, Mo.	115	6.02	0.052	565	2.01	0.041	889	1.53	0.048
Cairo, Ill.	199	3.57	0.046	753	1.84	0.040	1,150	1.50	0.045
Wytheville, Va.	63.1	8.66	0.060	364	2.88	0.061	607	2.06	0.078
Nashville, Tenn.	178	3.82	0.047	571	1.92	0.035	757	1.74	0.039
Knoxville, Tenn.	139	4.18	0.051	555	2.15	0.038	896	1.70	0.043
Charlotte, N.C.	147	4.78	0.057	480	2.21	0.038	660	1.88	0.031
Memphis, Tenn.	212	3.30	0.048	652	1.83	0.041	904	1.75	0.045
Chattanooga, Tenn.	204	3.20	0.051	604	1.89	0.033	851	1.72	0.033
Greenville, S.C.	182	3.72	0.047	702	2.16	0.037	998	2.19	0.045
Little Rock, Ark.	236	3.26	0.044	738	1.81	0.040	953	1.82	0.048
Columbia, S.C.	123	5.85	0.055	529	2.45	0.040	736	2.16	0.038
Atlanta, Ga.	213	3.36	0.046	699	1.99	0.037	961	1.89	0.040
Birmingham, Ala.	285	2.72	0.045	809	1.72	0.033	1,120	1.60	0.036
Augusta, Ga.	179	4.26	0.050	649	2.11	0.034	912	1.86	0.031
Macon, Ga.	203	3.68	0.047	795	1.80	0.032	1,220	1.64	0.041
Shreveport, La.	239	3.43	0.046	685	2.06	0.041	903	1.85	0.053
Vicksburg, Miss.	281	2.73	0.051	995	1.60	0.047	1,420	1.59	0.058
Montgomery, Ala.	298	2.83	0.042	1,020	1.56	0.039	1,380	1.55	0.052
Meridian, Miss.	348	2.57	0.041	885	1.75	0.032	1,130	1.80	0.041
Savannah, Ga.	324	3.02	0.044	1,240	1.46	0.035	1,800	1.29	0.041
Thomasville, Ga.	316	3.01	0.044	952	1.60	0.028	1,260	1.46	0.035
Jacksonville, Fla.	362	2.69	0.047	1,110	1.51	0.029	1,500	1.32	0.046
Pensacola, Fla.	463	2.35	0.036	1,660	1.36	0.043	2,470	1.26	0.057
New Orleans, La.	470	2.42	0.037	1,520	1.35	0.052	2,140	1.25	0.070

Table 7.---Standard errors for the single-coefficient, synthetic flood relation

Rain-gage location	Standard error in percent for various levels of imperviousness											
	2-yr recurrence interval				25-yr recurrence interval				100-yr recurrence interval			
	0	15	30	45	0	15	30	45	0	15	30	45
Dubuque, Iowa	22.2	15.2	13.3	12.0	13.2	12.2	10.2	8.7	11.4	13.1	12.3	10.9
Chicago, Ill.	21.0	14.6	12.4	11.0	11.9	11.0	9.0	7.7	10.1	11.6	11.0	10.5
Peoria, Ill.	18.8	13.2	10.9	9.5	11.5	10.0	8.8	7.5	13.5	11.3	11.3	10.9
Springfield, Ill.	19.8	13.7	11.0	9.1	11.2	9.8	8.3	7.1	10.5	8.6	7.6	6.8
Atlantic City, N.J.	18.3	13.1	10.9	9.4	12.7	12.5	10.7	9.3	13.0	15.4	14.6	13.4
Baltimore, Md.	21.1	14.1	11.2	9.6	16.0	14.0	13.3	13.1	15.7	15.0	14.8	14.4
Kansas City, Mo.	25.0	16.3	13.5	12.0	12.4	10.8	10.0	9.7	10.6	10.7	10.8	10.9
Columbia, Mo.	20.3	13.9	11.4	9.8	12.1	9.5	8.1	7.5	13.8	9.6	8.3	8.0
St. Louis, Mo.	19.1	13.2	10.5	8.7	8.6	8.5	7.5	6.6	8.2	8.3	8.2	7.8
Louisville, Ky.	17.5	13.6	12.1	11.1	10.4	8.6	7.9	6.9	12.2	8.5	10.2	10.6
Richmond, Va.	23.2	15.5	13.3	12.1	16.7	14.7	13.4	13.5	14.9	15.3	13.8	12.7
Lynchburg, Va.	24.1	14.9	11.7	9.6	17.6	13.6	11.8	12.0	15.9	14.5	12.4	11.3
Springfield, Mo.	22.0	14.0	11.4	9.5	11.2	11.1	9.6	8.0	11.1	13.0	13.1	12.1
Cairo, Ill.	15.4	12.4	10.4	8.8	9.5	9.7	9.4	8.8	9.5	10.3	11.2	11.0
Wytheville, Va.	24.4	15.8	12.7	10.8	17.6	15.3	14.2	13.8	21.2	19.1	17.7	16.7
Nashville, Tenn.	15.5	12.7	11.1	9.7	10.2	9.6	9.2	8.2	11.5	10.0	9.6	8.8
Knoxville, Tenn.	17.4	14.4	13.3	12.7	10.3	9.6	8.7	7.8	11.0	10.6	10.1	9.0
Charlotte, N.C.	19.6	14.6	12.4	10.8	12.2	10.2	8.6	7.3	10.6	8.1	7.8	7.2
Memphis, Tenn.	14.9	12.9	11.6	10.6	9.5	10.0	10.5	10.3	9.0	9.7	10.9	11.1
Chattanooga, Tenn.	16.6	14.7	13.7	13.1	10.8	8.9	8.4	7.9	9.8	8.2	7.9	7.7
Greenville, S.C.	15.5	12.8	11.0	9.4	10.3	9.9	9.2	9.1	14.0	14.5	15.0	15.3
Little Rock, Ark.	15.1	11.6	9.7	8.1	9.1	9.4	9.7	9.6	10.6	10.5	11.7	12.5
Columbia, S.C.	23.7	15.0	12.0	10.3	12.2	10.7	10.0	9.9	9.9	9.9	10.1	9.9
Atlanta, Ga.	15.6	12.4	10.5	9.0	9.6	8.9	8.4	8.0	11.3	10.0	9.8	9.8
Birmingham, Ala.	13.9	11.9	10.4	9.1	9.6	8.5	8.0	7.5	10.5	9.0	7.9	7.0
Augusta, Ga.	18.1	13.3	10.9	9.5	9.8	8.6	7.8	7.4	9.4	8.0	7.6	7.4
Macon, Ga.	15.7	12.4	10.2	8.4	7.7	8.1	7.7	7.0	9.3	9.6	10.0	9.9
Shreveport, La.	16.7	12.0	9.7	8.5	10.1	10.0	9.7	9.4	13.0	12.6	12.5	13.5
Vicksburg, Miss.	15.1	13.4	12.2	11.1	11.3	11.3	11.1	11.0	15.4	14.2	13.8	12.4
Montgomery, Ala.	13.9	11.2	9.3	7.6	8.4	9.3	9.7	9.5	11.4	11.8	12.6	12.4
Meridian, Miss.	13.1	10.8	9.0	7.5	7.5	7.8	7.7	7.3	11.1	10.3	10.7	10.9
Savannah, Ga.	14.9	11.6	10.4	10.2	7.7	8.0	8.5	8.8	9.1	8.8	9.7	10.5
Thomasville, Ga.	14.7	11.7	10.3	9.6	6.3	6.8	7.5	7.6	7.9	7.2	8.7	9.4
Jacksonville, Fla.	14.3	12.0	10.6	9.8	7.7	7.0	7.2	7.7	10.8	10.2	10.9	12.3
Pensacola, Fla.	10.9	9.3	8.1	7.1	9.8	10.1	10.2	10.1	14.7	14.0	13.9	13.8
New Orleans, La.	11.7	9.6	8.3	7.4	11.5	12.0	12.3	12.4	16.2	16.4	16.5	16.3